High-Nuclearity Metal–Organic Nanospheres: A Cd_{66} Ball

Stephen P. Argent,[†] Alex Greenaway,[†] Maria del Carmen Gimenez-Lopez,[†] William Lewis,[†] Harriott Nowell,[‡] Andrei N. Khlobystov,[†] Alexander J. Blake,[†] Neil R. Champness,*[,†] and Martin Schröder*[,†]

[†]School of Chemistry, University of Nottingham, University Park, Nottingham NG7 2RD, U.K.

[‡]Diamond Light Source, Diamond House, Harwell Science and Innovation Campus, Didcot, Oxfordshire OX11 0DE, U.K.

ABSTRACT: Reaction of H_3L with $Cd(NO_3)_2{\cdot}4H_2O$ in DMF at 150 °C for 3 days affords the metal–organic nanosphere $[Cd_{66}(\mu_3\text{-}OH)_{28}(\mu^3\text{-}O)_{16}(\mu^5\text{-}NO_3\text{-}O,O,O',O',O'',O'')_{12}(L)_{20}(\mu^2\text{-}DMF)_{12}\subset(DMF)_9]$. The cluster is composed of a spherical shell of 66 Cd(II) cations bridged by 28 μ^3-hydroxide, 16 μ^3-oxo, and five μ^5-NO_3– anions surrounded by a shell of 20 tripodal capping ligands (L) and 12 DMF ligands. The 66 Cd(II) cations and 12 NO_3– anions form a polydeltahedron that has 78 vertices [Cd(II) or NO_3–] (V), 228 edges (E), and 152 triangular faces (F), giving it an Euler characteristic (χ) of 2 ($\chi = V + F – E$). Reaction of H3L with $Cd(NO_3)_2{\cdot}4H_2O$ at lower temperatures or with $CdCl_2$ affords coordination polymer frameworks instead of nanospheres.

The synthesis of high-nuclearity transition-metal coordination clusters has been the focus of much research over recent years because of interest in tailoring the properties of nanoscale objects. Notable targets are the assembly of clusters and cages incorporating cavities that can act as hosts for guest species (1) as well as clusters, such as polyoxometalates, that have unusual electronic properties. (2) Thus, depending on their shape and composition, large clusters have found relevance in the areas of single-molecule magnets, (3) molecular electronics, (4) and host–guest chemistry (1, 5) and are a target for bottom-up nanoscale fabrication techniques. (6) Despite all of their potential applications, large clusters are often most admired for their attractive architectures and topologies. (7) Large clusters described in the literature have exhibited structural motifs reminiscent of zeolites, (8) fullerenes, (9)Platonic and Archimedean solids, (10) and viruses. (11)

One strategy employed to prepare high-nuclearity clusters is to incorporate ligands that act as caps while also encouraging the bridging of metal centers via co-ligands or anions. In this regard, comparisons can be made to the widely studied field of metal–organic framework

materials, (12) where ligand design is paramount in encouraging the assembly of arrays of metal centers and/or cluster building blocks. The use of polydentate ligands has been a frequently employed strategy in the synthesis of large d- and f-block clusters. Typically, small ligands such as triethanolamine, (13) iminocarboxylates, (14) epoxysuccinic acid, (15) and threonine are employed, (16) as they have a high degree of freedom and can rearrange their donor atoms to suit the stereoelectronic requirements and preferences of the metal ions. More heavily designed ligands incorporating binding units via pendant linkers impart structural information to the ligand shape *via* preorganization, which in turn influences directed cluster formation. (17) Reducing the degree of rigidity in these linkers increases the entropic price paid upon complexation but enhances flexibility and serendipity, which are crucial factors in the discovery of energetically favorable structures. (1)

H_3L (Figure 1a) was conceived and designed as an ambivalent nonplanar tecton that can twist to reduce potential phenyl–phenyl C–H interactions. It can thus potentially bind to metal centers either in an *endo* fashion via three carboxylates on the same trigonal face (to stabilize high-nuclearity clusters) or in an *exo* manner (to generate coordination polymers). We report herein the reproducible and designed synthesis and full characterization of a highly unusual Cd_{66} cluster, **1**, a high-nuclearity system incorporating a unique dual-shell structure (Figure 1) comprising a central inorganic Cd–oxo–hydroxy–nitrate cluster core surrounded by an organic shell of ligands. **1** contains ca. 1238 non-hydrogen atoms and has a molecular weight of ca. 23 800 Da. The pseudospherical ball has an external diameter of 3.18 nm (18) and an internal diameter of 1.22 nm (19) and thus can be considered a metal–organic nanosphere. (20) Interestingly, reaction of H_3L with Cd(II) salts under less vigorous conditions affords coordination polymers, whose syntheses can be controlled to form 1D, 2D, or 3D frameworks.

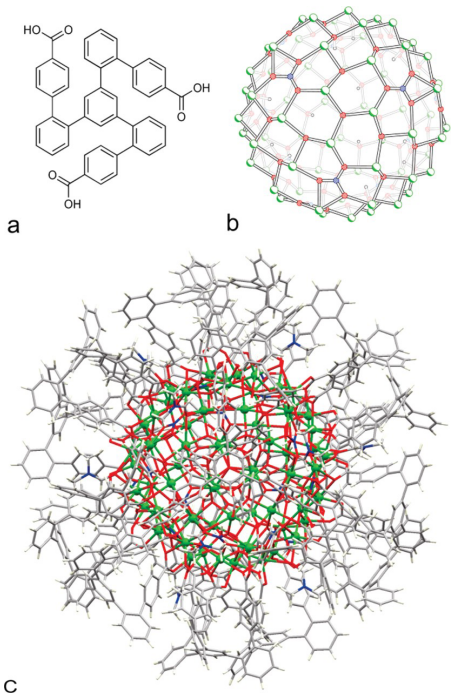

Figure 1. Views of (a) ligand H_3L, (b) the Cd–NO_3 core of **1** (carboxylate and DMF ligands omitted), and (c) **1**. Atom colors (all figures): C, gray; H, white; N, blue; O, red; Cd, green.

A solution of H_3L and $Cd(NO_3)_2{\cdot}4H_2O$ in *N*,*N*-dimethylformamide (DMF) was heated solvothermally at 150 °C for 3 days to give **1** as colorless parallelepipeds. Single-crystal X-ray analysis revealed **1** to be a cluster with the formula $[Cd_{66}(\mu^3\text{-}OH)_{28}(\mu^3\text{-}O)_{16}(\mu^5\text{-}NO_3\text{-}O,O,O',O',O'',O'')_{12}(L)_{20}(\mu^2\text{-}DMF)_{12}{\subset}(DMF)_9]$. **1** is composed of a spherical shell of 66 Cd(II) cations bridged by 28 μ^3-hydroxide, 16 μ^3-oxo, and 5 μ^5-NO_3^- anions (Figure 1b) surrounded by a shell of 20 tripodal capping ligands (L^{3-}) and 12 DMF ligands. **1** crystallizes in the trigonal space group $R\bar{3}$, and the cluster has C_3 crystallographic symmetry and idealized chiral tetrahedral *T* symmetry. However, each crystal is a racemate, with chiral molecules of **1**of both hands found in the unit cell.

A dual-shell structure for cluster **1** in which a central inorganic core is covered by an organic layer of L^{3-} ligands can readily be observed (Figure 1c). The 66 Cd(II) cations can be divided into six groups of centers with identical idealized symmetry: groups (i)–(v) each contain 12 centers showing a distorted octahedral coordination geometry, and group (vi) contains six centers having a biscapped square-pyramidal geometry [see the Supporting Information (SI)]. The six groups of Cd(II) cations differ in the make-up of their coordination spheres, which consist of varying combinations of carboxylate, hydroxide, oxo, nitrate, and DMF ligands. Within the groups of Cd(II) cations with identical idealized symmetry are centers with different crystallographic symmetry and hence differing coordinate bond lengths, though for the most part correlations between the geometries in these groups can be seen

(Table S3 in the SI). The octahedrally coordinated centers are all bound by either two or three carboxylate ligands and by two or three oxo/hydroxide ligands, with the remaining sites occupied by nitrate or DMF ligands. The biscapped square-pyramidally coordinated Cd(II) cations are all bound by two carboxylate ligands and two chelating nitrate anions resulting in centers with approximate C_{2v} symmetry.

The NO_3^- anions lie parallel to the surface of the spherical inorganic core, and each bridges five Cd(II) centers (Figure 2c).Identification of the 28 HO^- and 16 O^{2-} anions in the structure was determined by charge-balancing considerations to give an overall neutral species. Over the 16 crystallographically unique oxygen sites, the locations of HO^- groups were found by considering the observed Cd–O bond lengths and peaks in the crystallographic electron density map. Six of the O atoms (five full and one one-third occupancy) have average Cd–O bond lengths longer than the global mean value and have electron density peaks suggesting their assignment as HO^- groups. Four more HO^- sites are expected but could not be clearly distinguished from the spread of mean Cd–O bond lengths at the remaining sites. Thus, the HO^- sites are disordered among the remaining O^{2-} atoms. All HO^- and O^{2-} groups act as μ^3-ligands bridging three Cd(II) cations and project into the center of the sphere (Figure S2 in the SI). Within the inorganic shell, peaks were observed in the electron density map but could not be successfully modeled. SQUEEZE (21) was applied to the data to confirm that this 861 $Å^3$void contains 383 electrons, suggesting the presence of approximately nine small solvent molecules assigned as DMF. In the organic shell, the ligands and DMF molecules sterically block the entire surface of the metallo core except for small clefts through which NO_3^-anions are visible.

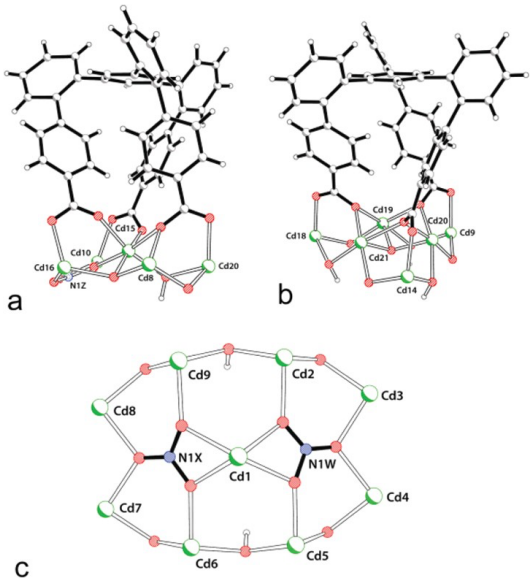

Figure 2. Views of the coordination environments of (a) ligand A at a threefold-symmetric site, (b) ligand D at a nonsymmetric site, and (c) nitrate anions W and X (carboxylate and DMF ligands omitted).

In the idealized *T* symmetry of the cluster, there are two ligand environments (Figure 2): eight ligands (A, B, G, H; Figure 2a) sit at the corners of a cubic array at positions of threefold symmetry bridging a triangle of three symmetry-related Cd(II) cations, and 12 ligands (C, D, E, F; Figure 2b) sit on the edges of the cubic array and bind to one central Cd(II) via their three carboxylate groups. The two types of ligand have opposing twist: clockwise for the eight threefold-symmetric ligands and anticlockwise for the remaining 12 ligands.

The 66 Cd(II) atoms and 12 NO_3^- anions can be viewed as the vertices of a polydeltahedron (Figure 3). The Cd vertices are all six-connected with Cd···Cd separations ranging from 3.49 to 3.99 Å, with the NO_3^- anions five-connected to Cd(II) centers (Cd···N separations ranging from 2.74 to 3.33 Å). Importantly, the 12 NO_3^- vertices are the precise number of five-coordinate defects necessary to allow the 66 six-coordinate vertices to enclose a sphere, as stated by Euler's theorem. (22) Thus, the convex polyhedron has 78 vertices [Cd(II) and NO_3^-] (V), 228 edges (E), and 152 triangular faces (F), giving it a closed-shell Euler characteristic (χ) of 2 ($\chi = V + F - E$).

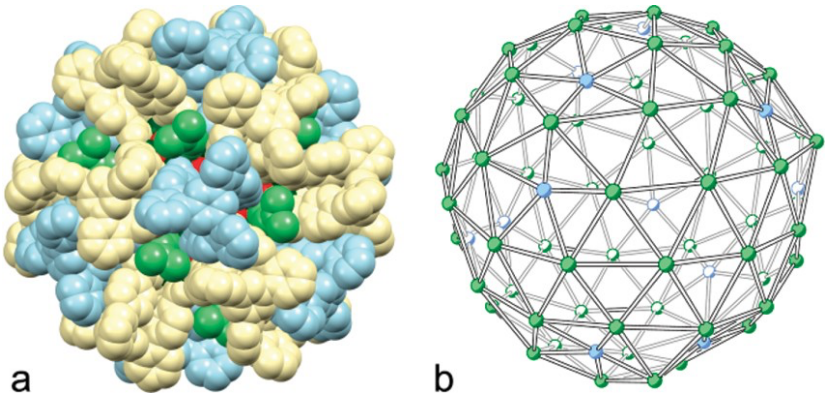

Figure 3. (a) Space-filling view of **1**. Colors: Ligand, blue and yellow; DMF, green. (b) Polydeltahedron formed by **1** based upon 66 Cd(II) centers (green) and 12 NO_3^- anions (blue) as vertices.

The solid-state packing in **1** is defined by hexagonal sheets of balls (centroid–centroid separations ranging from 3.55 to 4.09 nm) running parallel to the (110) plane to give sheets stacking in an ABAB pattern (plane separation of 2.89 nm). The stacking does not give a hexagonal close-packed structure because the spheres do not lie above and below the triangular pockets of the layers; instead, each sphere lies approximately halfway between two spheres from the layer above and layer below (separations of 3.52 and 3.55 nm) with a longer distance to the two next closest spheres (both 4.09 nm) (see the SI).

The synthesis of **1** is entirely reproducible: multiple batches of the Cd_{66} nanosphere complex were prepared from separate batches of H_3L, resulting in the exclusive formation of uniform crops of

parallelepipeds of **1** as confirmed by elemental analysis, NMR spectroscopy, mass spectrometry, and X-ray diffraction, which gave the correct unit cell dimensions for **1**. Crystals of a different solvate of the Cd_{66} sphere, **1a**, were prepared under identical conditions but using 1,4-dioxane as a cosolvent along with DMF. The structure of **1a** was refined in the space group *Pnnn* with the asymmetric unit containing only a quarter of the molecule (see the SI for further discussion).

1 is only sparingly soluble in several organic solvents, including $CHCl_3$, C_6H_5Me, and C_6H_6. The ^1H NMR spectrum recorded in CD_2Cl_2 features broad overlapping peaks in the 9.25–5.75 ppm region. Nine peaks of varying intensity can be discerned, and these are spread over a larger range than for the free ligand H_3L (7.95–6.62 ppm). Identical ^1H NMR spectra were observed for samples of **1** prepared from four different batches of H_3L. The broad nature of these peaks is consistent with the ligands being part of a large species with restricted tumbling in solution. ^1H NMR spectra of **1** in toluene-d_8 collected at temperatures ranging from 298 to 363 K showed few changes: one broad feature disappeared and minor changes occur in the chemical shifts of others, indicating little chemical change over the temperature range studied. The MALDI mass spectrum of a sample of **1** deposited from a CH_2Cl_2 solution featured a very broad peak spread over the range *m/z* 21800–23800. The minimum expected spread of mass spectral peaks for intact, **1** given the isotope pattern for 66 cadmium atoms, would be ca. *m*/*z* 100 (see the SI). The X-ray structure gives an average electron count for the encapsulated contents of the inorganic core. Although assigned to nine molecules of DMF, variations in content from cluster to cluster are likely. Additionally, even the mild conditions of MALDI could readily displace any number of the 12 surface-bound DMF ligands. Thus, a peak spread of *m*/*z* 1533, equivalent to 21 DMF molecules, combined with the resolution limitations of the technique, explains the broadness of the observed mass spectral peak. Further evidence for the persistence of **1** in solution was provided by dynamic light scattering (DLS) measurements in $CHCl_3$, which indicated the presence of a species with a diameter of 2.9 ± 1.1 nm.

The large size of **1** allowed its characterization and direct visualization using high-resolution transmission electron microscopy (TEM). A sample of **1** was deposited from $CHCl_3$ solution onto a copper-grid-mounted lacy carbon film. TEM images confirmed the presence of particles of a range of sizes encompassing that expected for the intact complex (see the SI). The distribution of sizes suggests that the molecules were damaged by the electron beam, so a sample of **1** was subsequently deposited from chloroform solution into multiwalled carbon nanotubes (MWNTs) prior to imaging. MWNTs have previously been used as transparent test tubes for visualizing molecular clusters using TEM, acting as an electromagnetic shield and a heat and charge sink to minimize the detrimental effects of the electron beam on the sample. (23)Molecules of **1** imaged inside MWNTs showed consistently good

agreement with the size expected for intact clusters (Figure 4). The presence of cadmium in the species imaged by TEM both on carbon films and inside MWNTs was confirmed by localized energy-dispersive X-ray (EDX) spectroscopy.

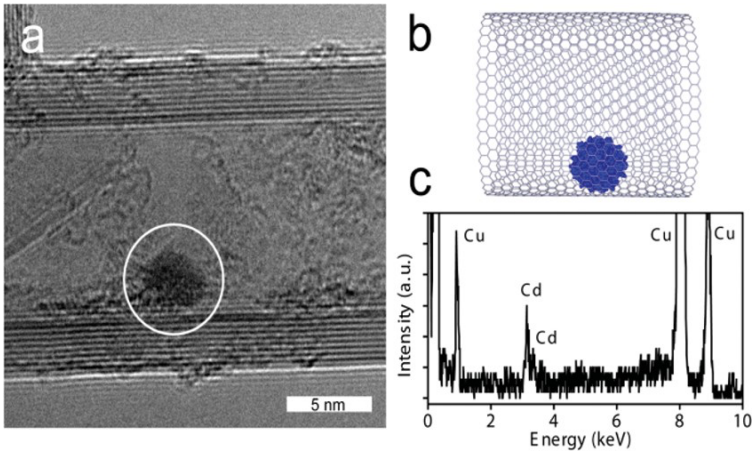

Figure 4. (a) Conventional bright-field TEM image of **1** inserted into a nanotube (scale bar is 5 nm). (b) Schematic representation of (a). (c) EDX spectrum of the selected area in the nanotube (circle), confirming the presence of Cd-containing molecules within the nanotube (Cu peaks are due to the copper TEM support grid).

To probe the conditions necessary for the formation of **1**, reactions were carried out at lower temperatures under various conditions and with $CdCl_2$ instead of $Cd(NO_3)_2{\cdot}4H_2O$. These lower-energy experiments afforded the 1D and 2D coordination frameworks **2**, **3**, and **4** (see the SI).

Thus, diffusion of diisopropyl ether into a solution of H_3L and $Cd(NO_3)_2{\cdot}4H_2O$ in DMF and 1,4-dioxane at room temperature resulted in a crop of colorless crystals whose single-crystal X-ray structure revealed a 1D coordination polymer $[Cd_3(L)_2(DMF)_5(H_2O)_2]_\infty$, **2**. In **2**, pairs of tricarboxylic L^{3-} ligands in tripodal conformations sandwich triangular arrays of three Cd(II) cations (Cd–Cd separations of 7.89–8.14 Å) with each carboxylate group chelating to one Cd(II) cation in a η^2-fashion. Adjacent $[Cd_3(L)_2]$ moieties are bridged in an anti conformation by pairs of chelated carboxylates, resulting in the formation of Cd_2O_2 squares.

Reaction of H_3L with $Cd(NO_3)_2{\cdot}4H_2O$ in DMF at an intermediate temperature of 80 °C for 2 weeks yielded colorless, thin, platelike crystals. X-ray analysis revealed a 2D coordination framework, $[Cd_3(L)_2(DMF)_4]_\infty$, **3**, composed of linear $[Cd_3(RCO_2)_6(DMF)_4]$ clusters, with each carboxylate ligand bridging three clusters to form 2D sheets. In contrast to the tripodal conformation adopted in **1** and **2**, two of the arms of L^{3-} in **3** project above the plane of the central phenyl ring and one lies below.

To assess the role of the NO_3^- anions, H_3L was treated with $CdCl_2$ in DMF at 150 °C for 3 days. Colorless crystals were obtained, and their structure was revealed by X-ray analysis to be $\{[Cd_3Cl(L)_2(DMF)(Me_2NH)]Me_2NH_2\}_\infty$, **4**. This 2D coordination framework is composed of $[Cd_3Cl(RCO_2)_6]$ clusters bridged via six different ligands, resulting in sheets of **kgd** topology, identical to the topology observed for **3**. Within the Cd_3Cl cluster, the Cl^- anion is bound to three Cd(II) cations arranged in a T-shaped geometries. (24)

In conclusion, we have successfully demonstrated the synthesis and characterization of a highly unusual high-nuclearity Cd_{66} metal–organic nanosphere. Our strategy leads to the formation of a dual-shell cluster consisting of an inorganic shell built from Cd(II) cations and O^{2-}, HO^-, and NO_3^- anions capped by an organic shell of tricarboxylate and DMF ligands. The cluster forms a unique polydeltahedron that also encompasses a large void space with a diameter of over 1 nm containing nine DMF molecules. Reactions at lower temperatures suggested the presence of a large thermodynamic barrier that must be overcome to form nanospheres, while reactions in the absence of NO_3^- anions confirmed that the presence of this anion is needed to template the formation of nanospheres. Future work seeks to develop and investigate new methodologies for the synthesis of complex high-nuclearity metal nanoclusters and aggregates.

ASSOCIATED CONTENT

Supporting Information

Single-crystal X-ray structures, experimental details, character-
ization data, and NMR and mass spectra. This material is available free of charge via the Internet at http://pubs.acs.org.

AUTHOR INFORMATION

Corresponding Author

m.schroder@nottingham.ac.uk; neil.champness@nottingham. ac.uk

ACKNOWLEDGMENTS

This work was supported by the ERC, the EPSRC, and the University of Nottingham. M.S. gratefully acknowledges an ERC Advanced Grant and an EPSRC Programme Grant.

N.R.C. gratefully acknowledges a Royal Society Leverhulme Trust Senior Research Fellowship and a Royal Society Wolfson Merit Award. We thank Victoria J. Richards for help in determining network topologies using TOPOS,25 Dr. Sihai Yang for collecting XRPD data, and Dr. Graham Rance for assistance with DLS measurements. We also acknowledge the EPSRC National Service for Mass

Spectrometry at the University of Swansea for assistance in mass spectrometric analysis and Diamond Light Source for access to Beamline I19.

REFERENCES

(1) Ward, M. D. Chem. Commun. 2009, 4487.

(2) (a) Müller, A.; Beckmann, E.; Bögge, H.; Schmidtmann, M.; Dress, A. Angew. Chem., Int. Ed. 2002, 41, 1162. (b) Fleming, C.; Long, D.-L.; McMillan, N.; Johnson, J.; Bovet, N.; Dhanak, V.; Gadegaard, N.; Kögerler, P.; Cronin, L.; Kadodwala, M. Nat. Nanotechnol. 2008, 3, 229.

(3) (a) Kong, X.-J.; Ren, Y.-P.; Long, L.-S.; Zheng, Z.; Huang, R.-B.; Zheng, L.-S. J. Am. Chem. Soc. 2007, 129, 7016. (b) Bi, Y.; Wang, X.-T.; Liao, W.; Wang, X.; Wang, X.; Zhang, H.; Gao, S. J. Am. Chem. Soc. 2009, 131, 11650. (c) Christou, G.; Tasiopoulos, A. J. J. Am. Chem. Soc. 2010, 132, 16146.

(4) Bogani, L.; Wernsdorfer, W. Nat. Mater. 2008, 7, 179.

(5) (a) Moulton, B.; Lu, J.; Mondal, A.; Zaworotko, M. J. Chem. Commun. 2001, 863. (b) Perry, J. J. IV; Kravtsov, V. Ch.; McManus, G. J.; Zaworotko, M. J. J. Am. Chem. Soc. 2007, 129, 10076. (c) Suzuki, K.; Takao, K.; Sato, S.; Fujita, M. J. Am. Chem. Soc. 2010, 132, 2544.

(d) Mugridge, J. S.; Bergman, R. G.; Raymond, K. N. Angew. Chem., Int. Ed. 2010, 49, 3635. (e) Zhao, D.; Tan, S.; Yuan, D.; Lu, W.; Rezenom, Y. H.; Jiang, H.; Wang, L.-Q.; Zhou, H.-C. Adv. Mater. 2011, 23, 90.

(6) Pradeep, C. P.; Long, D.-L.; Streb, C.; Cronin, L. J. Am. Chem. Soc. 2008, 130, 14946.

(7) (a) Müller, A. Science 2003, 300, 749. (b) Chakrabarty, R.; Mukherjee, P. S.; Stang, P. J. Chem. Rev. 2011, 111, 6810.

(8) Kong, X.-J.; Wu, Y.; Long, L.-S.; Zheng, L.-S.; Zheng, Z. J. Am. Chem. Soc. 2009, 131, 6918.

(9) (a) Bai, J.; Virovets, A. V.; Scheer, M. Science 2003, 300, 781.

(b) Kong, X.-J.; Long, L.-S.; Zheng, Z.; Huang, R.-B.; Zheng, L.-S. Acc. Chem. Res. 2010, 43, 201.

(10) (a) Argent, S. P.; Adams, H.; Riis-Johannessen, T.; Jeffery, J. C.; Harding, L. P.; Mamula, O.; Ward, M. D. Inorg. Chem. 2006, 45, 3905.

(b) Argent, S. P.; Adams, H.; Harding, L. P.; Ward, M. D. Dalton Trans. 2006, 542. (c) Stephenson, A.; Argent, S. P.; Riis-Johannessen, T.; Tidmarsh, I. S.; Ward, M. D. J. Am. Chem. Soc. 2011, 133, 858.

(11) Liu, T.; Diemann, E.; Li, H.; Dress, A. W. M.; Müller, A. Nature 2003, 426, 59.

(12) (a) Hoskins, B. F.; Robson, R. J. Am. Chem. Soc. 1990, 112, 1546. (b) Eddaoudi, M.; Moler, D. B.; Li, H. L.; Chen, B. L.; Reineke,

T. M.; O'Keeffe, M.; Yaghi, O. M. Acc. Chem. Res. 2001, 34, 319.

(c) Champness, N. R. Dalton Trans. 2006, 877. (d) Uemura, T.; Yanai, N.; Kitagawa, S. Chem. Soc. Rev. 2009, 38, 1228. (e) Lin, X.; Telepeni, I.; Blake, A. J.; Dailly, A.; Brown, C.; Simmons, J.; Zoppi, M.; Walker,

G. S.; Thomas, K. M.; Mays, T. J.; Hubberstey, P.; Champness, N. R.; Schröder, M. J. Am. Chem. Soc. 2009, 131, 2159. (f) Yang, S.; Lin, X.; Blake, A. J.; Walker, G. S.; Hubberstey, P.; Champness, N. R.; Schröder, M. Nat. Chem. 2009, 1, 487. (g) Blake, A. J.; Champness, N. R.; Easun, T. L.; Allan, D. R.; Nowell, H.; George, M. W.; Jia, J.; Sun, X.-Z. Nat. Chem. 2010, 2, 688.

(13) Liu, T.; Zhang, Y.-J.; Wang, Z.-M.; Gao, S. J. Am. Chem. Soc.

2008, 130, 10500.

(14) (a) Doble, D. M. J.; Benison, C. H.; Blake, A. J.; Fenske, D.; Jackson, M. S.; Kay, R. D.; Li, W. S.; Schröder, M. Angew. Chem., Int. Ed. 1999, 38, 1915. (b) Lin, X.; Doble, D. M. J.; Blake, A. J.; Harrison, A.; Wilson, C.; Schröder, M. J. Am. Chem. Soc. 2003, 125, 9476.

(c) Kong, X.-J.; Ren, Y.-P.; Long, L.-S.; Zheng, Z.; Huang, R.-B.;

Zheng, L.-S. J. Am. Chem. Soc. 2007, 129, 7016. (d) Kong, X.-J.; Ren,

Y.-P.; Chen, W.-X.; Long, L.-S.; Zheng, Z.; Huang, R.-B.; Zheng, L.-S.

Angew. Chem., Int. Ed. 2008, 47, 2398. (e) Kong, X.-J.; Ren, Y.-P.;

Long, L.-S.; Zheng, Z.; Nichol, G.; Huang, R.-B.; Zheng, L.-S. Inorg. Chem. 2008, 47, 2728.

(15) Fang, S.-M.; Zhang, Q.; Hu, M.; Sanudo, E. C.; Du, M.; Liu, C.-S. Inorg. Chem. 2010, 49, 9617.

(16) Kong, X.-J.; Wu, Y.; Long, L.-S.; Zheng, L.-S.; Zheng, Z. J. Am. Chem. Soc. 2009, 131, 6918.

(17) (a) Caulder, D.; Brückner, C.; Powers, R.; König, S.; Parac, T.; Leary, J.; Raymond, K. J. Am. Chem. Soc. 2001, 123, 8923. (b) Bi, Y.; Wang, X.-T.; Liao, W.; Wang, X.; Wang, X.; Zhang, H.; Gao, S. J. Am. Chem. Soc. 2009, 131, 11650. (c) Ronson, T.; Fisher, J.; Harding, L.;

Rizkallah, P.; Warren, J.; Hardie, M. Nat. Chem. 2009, 1, 212. (d) Allen, K.; Faulkner, R.; Harding, L.; Rice, C.; Riis-Johannessen, T.; Voss, M.; Whitehead, M. Angew. Chem., Int. Ed. 2010, 49, 6655. (e) Tong, L. H.; Guenee, L.; Williams, A. F. Inorg. Chem. 2011, 50, 2450.

(18) Distance measured between centroids of diametric phenyl rings.

(19) Distance measured between hydroXide H atoms.

(20) Champness, N. R. Angew. Chem., Int. Ed. 2009, 48, 2274.

(21) (a) Spek, A. L. J. Appl. Crystallogr. 2003, 36, 7. (b) Sluis, P. v. d.; Spek, A. L. Acta Crystallogr. 1990, A46, 194.

(22) Bausch, A. R.; Bowick, M. J.; Cacciuto, A.; Dinsmore, A. D.; Hsu, M. F.; Nelson, D. R.; Nikolaides, M. G.; Weitz, A. T. Science 2003, 299, 1716.

(23) Gimeńez-Loṕez, M. C.; Moro, F.; La Torre, A.; Goḿez-García,

C. J.; Brown, P. D.; van Slageren, J.; Khlobystov, A. N. Nat. Commun.
2011, 2, No. 407.
(24) (a) Yi, L.; Ding, B.; Zhao, B.; Cheng, P.; Liao, D.-Z.; Yan, S.-P.; Jiang, Z.-H. Inorg. Chem. 2004, 43, 33. (b) Tong, X.-L.; Wang, D.-Z.; Hu, T.-L.; Song, W.-C.; Tao, Y.; Bu, X.-H. Cryst. Growth Des. 2009, 9, 2280.
(25) Blatov, V. A. CompComm Newsl. 2006, 7, 4.

Supporting Information

High Nuclearity Metal-Organic Nanospheres: A Cd_{66} Ball

Stephen P. Argent, Alex Greenaway, Maria del Carmen Gimenez-Lopez, William Lewis, Harriott Nowell, Andrei N. Khlobystov, Alexander J. Blake, Neil R. Champness* and Martin Schröder*

Synthesis

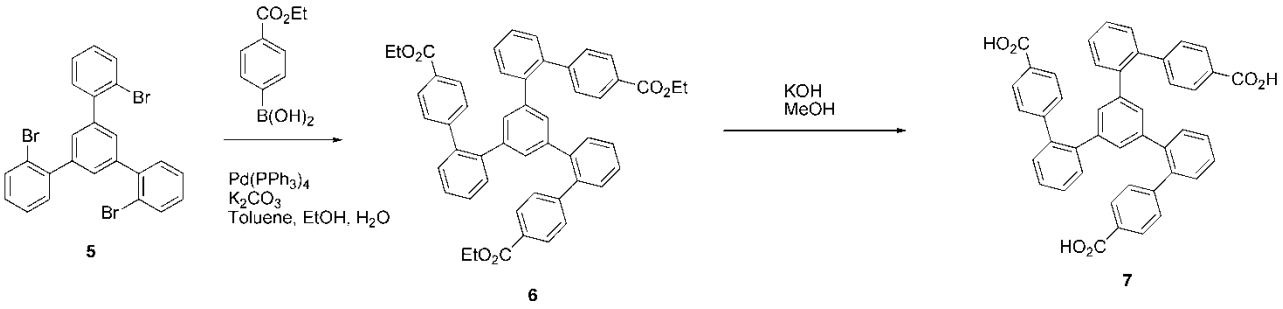

Scheme S1. Synthesis of **7**

Synthesis of 6

A Schlenk flask was charged with **5** (1.25 g, 2.30 mmol), 4-ethoxycarbonylphenylboronic acid (1.79 g, 9.21 mmol), K_2CO_3 (3.17 g, 23,0 mmol), toluene (60 cm^3), EtOH(10 cm^3) and water (10 cm^3). The flask was fitted with a condenser and the mixture degassed under N_2 at 80°C for 45 mins after which [$Pd(PPh_3)_4$] (53 mg, 0.0460 mmol) was added. The mixture was stirred at 80°C for 3 days. The reaction mixture was allowed to cool and diluted with toluene and water. The organic phase was separated and washed with further water and brine before being dried over $MgSO_4$. After removal of solvent the crude solid was purified by slow recrystallisation from $CHCl_3$ and MeOH to give **6** as large white crystals (1.05 g, 61%). ^{1}H-NMR (400 MHz, $CDCl_3$), 8.07 (6H, d, *J* 8.3), 7.41-7.36 (6H, m), 7.33-7.28 (3H, m), 7.03 (6H, d, *J* 8.2), 6.92 (3H, d, *J* 7.5), 6.72 (3H, s), 4.40 (6H, q, *J* 7.1), 1.41 (9H, t, *J* 7.1). ^{13}C-

NMR (500 MHz, $CDCl_3$) 166.41 (C=O), 146.27 (C), 140.89 (C), 140.16 (C), 139.57 (C), 130.52 (CH), 130.12 (CH), 130.09 (CH), 129.83 (CH), 129.34 (CH), 129.18 (CH), 128.57 (C), 127.94, 127.57 (CH), 60.97 (CH_2), 14.34 (CH_3). MS MALDI(+) (DCM, DCTB/MeCN) *m/z* 750.5 $[M]^+$, 773.5 $[M+Na]^+$, 789.5 $[M+K]^+$. Elemental analysis: Found (Required for $C_{51}H_{42}O_6$) C 81.09 (81.58), H 5.20 (5.64).

Synthesis of 7

The triester **6** (450 mg, 0.358 mmol) was suspended in a mixture of aqueous KOH (2 M, 25 cm^3) and MeOH (25 cm^3). The mixture was agitated by ultrasound before being heated under reflux for 2 days. The MeOH was removed from the solution which was then adjusted to *ca* pH 4 by addition of HCl (6 M). The resulting pale yellow precipitate of **7** was collected by centrifuge and washed with water (323 mg, 81%). ^{1}H-NMR (400 MHz, DMSO-d_6) 12.95 (3H, s-br), 7.98 (6H, d, *J* 8.6), 7.43 (3H, td, *J* 7.4, 1.1), 7.39 (3H, dd, *J* 7.6, 1.6), 7.34 (3H, td, *J* 7.4, 1.6), 7.02-6.95 (6H, m), 6.62 (3H, s). ^{13}C-NMR (400 MHz, DMSO-d_6) 167.4 (CO), 146.0 (C), 140.9 (C), 139.8 (C), 139.6 (C), 130.6 (C), 130.5 (CH), 130.4 (CH), 129.8 (CH), 129.5 (CH), 129.4 (CH), 128.6 (CH), 128.4 (CH). MS MALDI(-) (DMF, DCTB/MeCN) *m/z* 665.3 $[M-H]^+$. Elemental analysis: Found (Required for $C_{45}H_{30}O_6$) C 80.89 (81.07), H 4.43 (4.54).

Synthesis of 1 - $Cd_{66}(OH)_{28}(O)_{16}(NO_3)_{12}L_{20}(DMF)_{12}\subset(DMF)_9$

A solution of **7** (30.0 mg, 0.0450 mmol) and $Cd(NO_3)_2{\cdot}4H_2O$ (83.0 mg, 0.270 mmol) in DMF (15 cm^3) were heated solvothermally at 150°C for 3 days to give **1** as colorless parallelepidic crystals which were collected by filtration and dried *in vacuo* (yield 17.0 mg, 31%). Elemental analysis: Found (Required for $Cd_{66}(OH)_{28}(O)_{16}(NO_3)_{12}L_{20}(DMF)_{12}\subset(DMF)_9{\cdot}100(H_2O)$) C 45.35 (45.35), H 2.70 (3.62), N 1.63 (1.81).

Synthesis of 1a - $Cd_{66}(OH)_{28}(O)_{16}(NO_3)_{12}L_{20}(OR)_{12}\subset(DMF)_9$

A solution of **7** (3.00 mg, 0.00450 mmol) and $Cd(NO_3)_2{\cdot}4H_2O$ (8.32 mg, 0.0270 mmol) in a mixture of DMF (1.5 cm^3) and 1,4-dioxane (0.5 cm^3) were heated solvothermally at 150°C for 3 days to give **1a** as colorless columnar crystals.

Synthesis of 2 – [$Cd_3L_2(DMF)_5(H_2O)_2]_\infty$

Diisopropyl ether was slowly diffused into a solution of **7** (5.00 mg, 0.00750 mmol) and $Cd(NO_3)_2{\cdot}4H_2O$ (13.9 mg, 0.0450 mmol) in a mixture of DMF (1.50 cm^3) and 1,4-dioxane (1.00 cm^3) at room temperature to give **2** as colorless obelisks amongst amorphous white material. Individual crystals of **2** for single crystal X-ray analysis could be manually separated from the mixture.

Synthesis of 3 - $[Cd_3L_2(DMF)_4]_\infty$

A solution of **7** (3.00 mg, 0.00450 mmol) and $Cd(NO_3)_2{\cdot}4H_2O$ (8.32 mg, 0.0270 mmol) in DMF (1.5 cm^3) were heated at 80°C for 2 weeks to give **3** as colorless thin plates. Elemental analysis: Found (Required for $Cd_3L_2(DMF)_4$) C 62.48 (62.60), H 4.17 (4.22), N 3.11 (2.86).

Synthesis of 4 - $\{[Cd_3Cl(L)_2(DMF)(Me_2NH)Me_2NH_2]_\infty$

A solution of **7** (4.00 mg, 0.00600 mmol) and $CdCl_2$ (6.60 mg, 0.0360 mmol) in DMF (2 cm^3) were heated solvothermally at 150°C for 3 days to give **4** as colorless blocks. Elemental analysis: Found (Required for $Cd_3Cl(L)_2(DMF)(Me_2NH){\cdot}(Me_2NH_2)$) C 62.45 (62.49), H 3.95 (4.11), N 2.27 (2.25).

Transmission Electron Microscopy Experimental

Multiwalled carbon nanotubes (MWNT) produced by arc discharge were purchased from Mer Corporation. High-resolution transmission electron microscopy (TEM) imaging and energy-disperse X-ray (EDX) analyses were performed using a Jeol 2100F transmission electron microscope using an accelerating voltage of 100 kV. TEM samples were prepared by casting several drops of a suspension of the

complex in $CHCl_3$ onto copper-grid mounted lacey carbon film before drying under a stream of nitrogen.

Preparation of short and open MWNT via oxidative cutting.

MWNT (50 mg) were added to a concentrated solution of nitric acid (100 mL) and the resulting black suspension was treated with ultrasound in a water bath for 30 min at room temperature. The suspension was then heated in air under reflux for 2h. The resultant mixture was diluted with deionized water (200 mL), filtered using a 0.45 μm pore size PTFE membrane filter, washed thoroughly with water to neutral pH, and then washed further with EtOH (50 mL) and dried under vacuum to yield a black solid (45 mg). The product was placed in an alumina crucible and heated in air at 700°C for 20 min (weight loss of 60%).

Insertion of 1 into MWNT.

Freshly annealed MWNT (1 mg, short and open) were added to a solution of **1** (2 mg) in $CHCl_3$ (0.7 mL) at room temperature. The solvent was removed slowly by evaporation under vacuum, and an additional aliquot of $CHCl_3$ (0.4 mL) was added. The resultant mixture was stirred vigorously and the solvent evaporated again. This procedure was repeated a further two times. The resulting black powder was dispersed in $CHCl_3$ (0.4 mL) under ultrasonic agitation, filtered onto PTFE filtration membrane (pore size 0.2 μm), washed with $CHCl_3$ (5 mL) and dried in air.

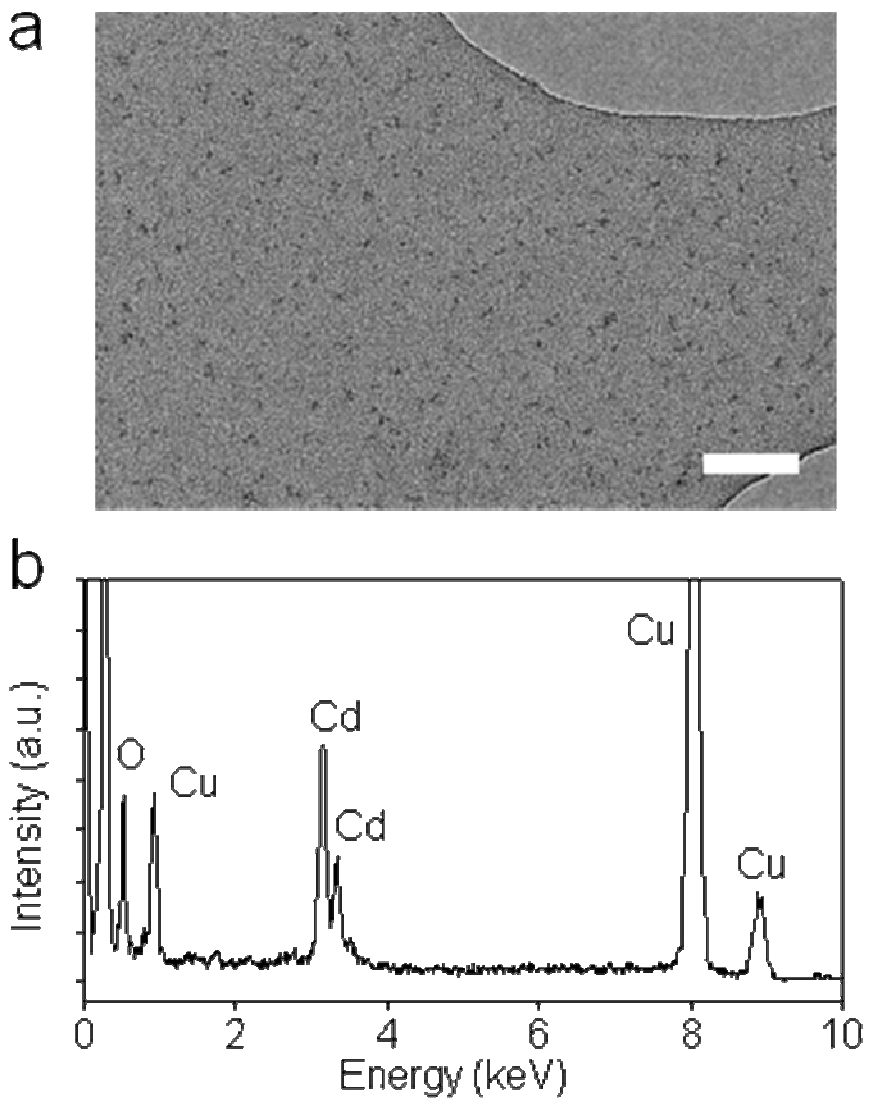

Fig. S1 a) Conventional bright field transmission electron micrographs of **1** (scale bar is 50 nm). b) EDX spectrum confirming the presence of Cd in **1** (Cu peaks are due to a copper TEM support grid).

Dynamic Light Scattering (DLS)

DLS was performed using a Malvern Instruments Nano-ZS Zetasizer at room temperature. An excess of **1** (*ca* 3 mg) was dispersed in $CHCl_3$ (2.5 mL) using sonication and the resultant solution/suspension was clarified by centrifugation and allowed to equilibrate for 20 mins. Measurements were also performed on neat $CHCl_3$ to ensure no impurities were present. Average particle diameters (APD) and their widths are quoted in units of nm. Quoted values are the average of 4 measurements.

DLS measurements on neat $CHCl_3$ showed one peak at 0.76(±0.16) nm attributable to the solvent molecules, while measurements on an equilibrated saturated solution of **1** in $CHCl_3$ reveal a peak at 2.9(±1.1) nm consistent with the presence of intact nanospheres (expected size 3.18 nm). Both of these very small peaks lie in a region where the accuracy of DLS is limited. The fit to the data for **1** in solution is impaired by very small quantities of larger species (only apparent in the intensity plot) which render the sample too polydispersed for in-depth quantitative analysis.

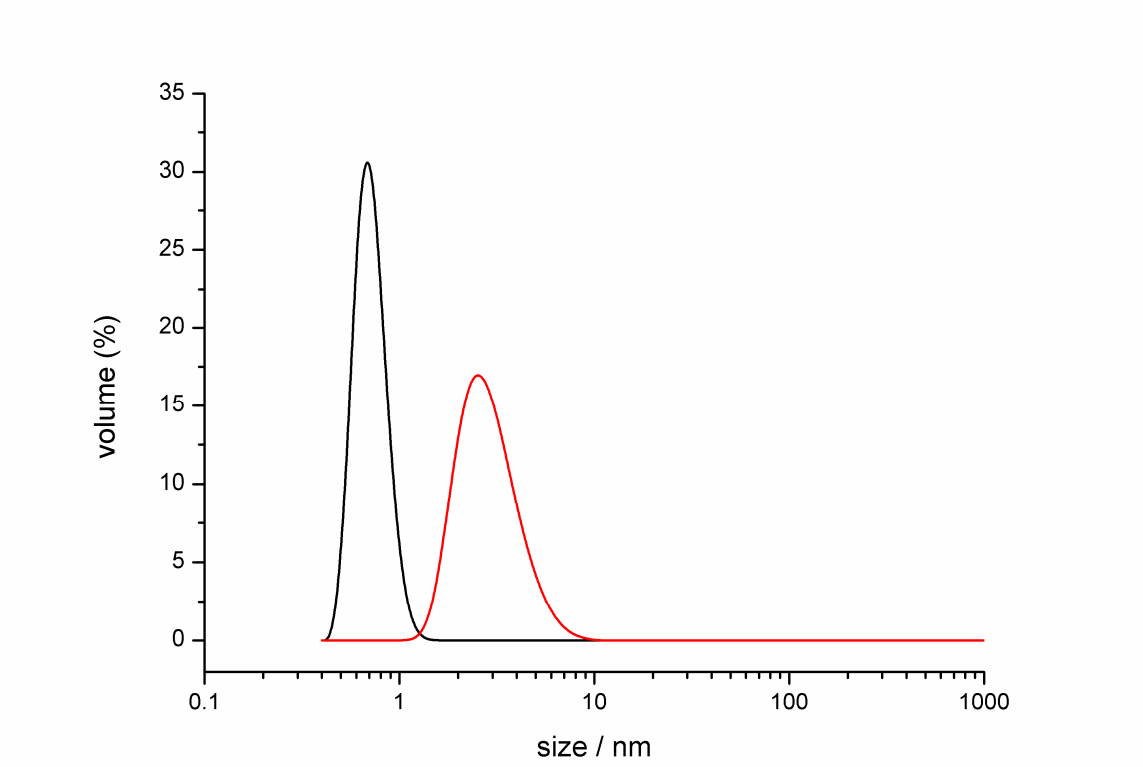

Fig. S2 DLS frequency plots for neat solvent [black, APD 0.76(±0.16) nm] and **1** dissolved in $CHCl_3$ [red, APD 2.9(±1.1)]. Both lines are averages of four measurements.

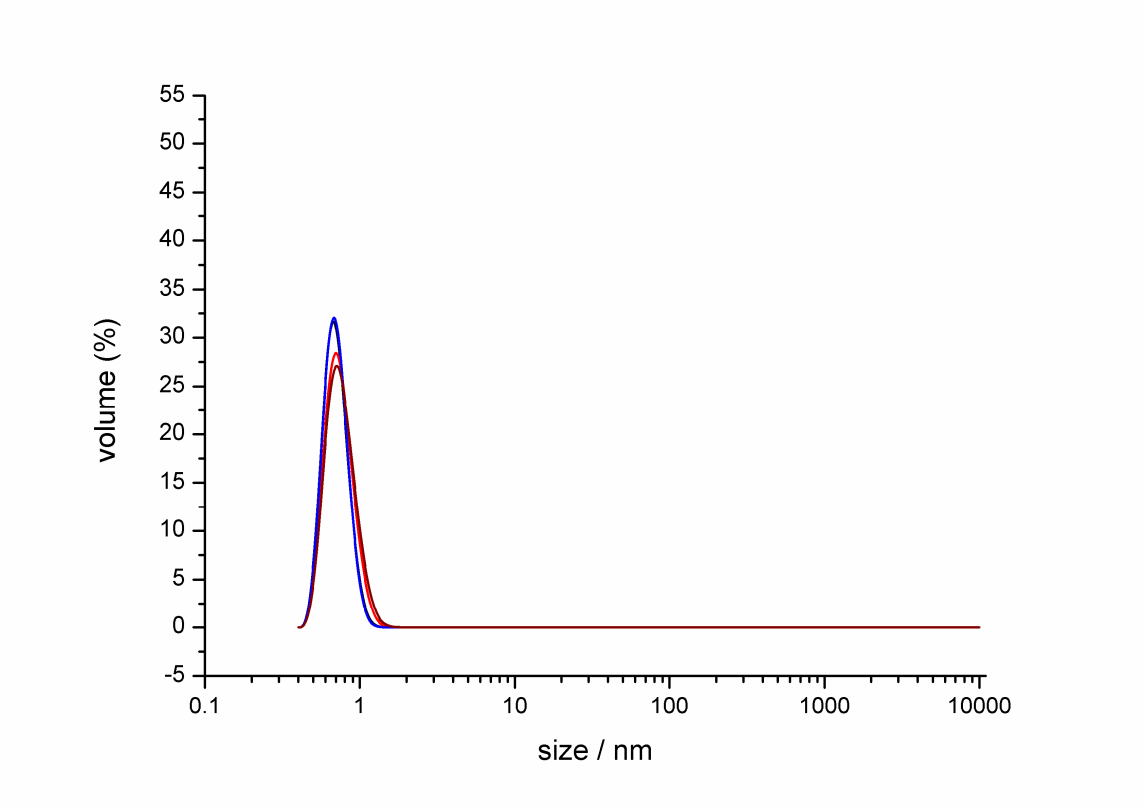

Fig. S3 DLS frequency plots for neat solvent with four individual measurements overlaid.

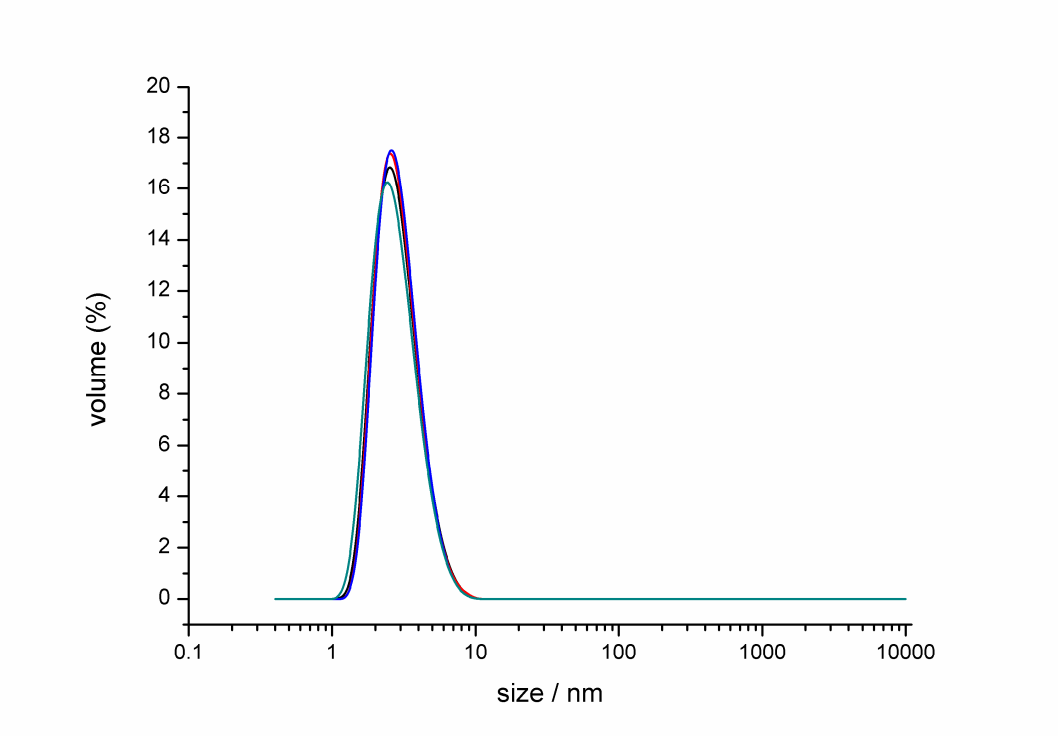

Fig. S4 DLS frequency plots for **1** dissolved in $CHCl_3$ with four individual measurements overlaid.

Single Crystal X-ray Structure of 1a

The single crystal X-ray structure of **1a** reveals the cluster to have the same gross structure and conformation as **1**. Complex **1a** crystallizes in orthorhombic space group *Pnnn* with one quarter of the complex in the asymmetric unit (Fig. S5). This is in contrast with **1** where one third of the complex is present. The other key difference between the two structures is the identity of the twelve capping μ^2-ligands in the organic sphere: in **1** these ligands are unambiguously DMF molecules whereas in **1a** these groups cannot be clearly identified. Attempts to model the electron density as various plausible decomposition products of DMF and 1,4-dioxane were unsuccessful. Ultimately the groups (which could not be treated by PLATON SQUEEZE) were modeled as several partially occupied carbon atoms binding *via* an oxygen atom. The similar co-ordination geometry of the oxygen atoms in **1a** and the bridging DMF ligands in **1** suggests that the unidentified species is also neutral. Of the 11 crystallographically unique oxygen atoms in the metallo core of **1a** it is required that seven of them be HO^- and four of them O^{2-}anions for the cluster to be neutral. Similar perturbations in Cd-O bond lengths and electron density peaks to those observed in **1** allowed the assignment of four of these oxygen atoms as being HO^- groups (O22, O29, O30, O31) (Tables S1 and S2). The residual electron density peaks within the metallo core could not be successfully modeled. The application of PLATON SQUEEZE to the data indicated that the void of 883 $Å^3$ contained 334 electrons.

Crystallographic Refinement Details

Complex 1

Rigid bond and similarity restraints (DELU, SIMU) have been applied to the anisotropic displacement parameters of all the dimethylformamide and carboxylate ligands. Similarity restraints (SADI, SAME) have been applied to the geometries of the free dimethylformamide molecules and carboxylate

ligands. The trisubstituted phenyl ring of each ligand has been constrained to have regular hexagonal geometry (AFIX 66), and dimethylformamide molecule P modelled at half-occupancy with isotropic displacement parameters. Rigid bond restraints (DELU) have been applied to the anisotropic displacement parameters of nitrate moieties X, Y and Z. The anisotropic displacement parameters of oxygen atom O4W have been restrained to have isotropic behaviour (ISOR), and the four nitrate moieties have each been restrained to lie in a flat plane (FLAT), while similarity restraints have been applied to their 1,2 and 1,3 separations to reflect their idealised 2-fold symmetry (SADI). Attempts to model these nitrate moieties as being disordered over two positions were unsuccessful.

To give a charge-balanced structure required that 9 1/3 of the 14 2/3 oxygen atoms in the asymmetric unit be hydroxide ligands with the remainder being oxo ligands. Observation of hydrogen atom peaks in the electron density map combined with longer Cd-O bond lengths confirmed the identity of 5 1/3 oxygen atoms as hydroxide ligands (O25, O28, O31, O34, O35 and O36). The hydrogen atoms for these ligands were geometrically placed to make an equal angle with each O-Cd bond (AFIX 13) and refined using a riding model. The location of the remaining four hydroxide groups could not be determined and were not included in the model but were included in the unit cell contents. There are no acceptors for these hydrogen donor groups as the species which these groups are likely to donate to are disordered and have been suppressed by the PLATON SQUEEZE function (see below).

The contents of the large internal cavity of the molecule were disordered and could not be modeled. Consideration of the output of PLATON SQUEEZE (see below) indicated an electron count of 383 in a void of volume 855 A^3. These data are consistent with the cavity being occupied by 9 dimethylformamide molecules (3 per symmetric unit). Some large residual electron density peaks remain in the void even after refinement of the structure against the solvent-free diffraction data generated by PLATON SQUEEZE.

PLATON SQUEEZE has been applied to the data to remove the scattering contribution from several

disordered solvent moieties and produce a set of solvent-free diffraction intensities for the final cycles of refinement. A total of 25274 electrons were removed from the P1 cell, equating to around 104 dimethylformamide molecules per asymmetric unit which have been included in the unit cell contents.

Complex 1a

Rigid bond and similarity restraints (DELU, SIMU) have been applied to the anisotropic displacement parameters of all atoms in the structure. Similarity restraints (SADI, SAME) have been applied to the geometries of the carboxylate ligands. The trisubstituted phenyl ring of each ligand has been constrained to have regular hexagonal geometry (AFIX 66). The nitrate moieties have been restrained to lie flat (FLAT) and the 1,2 separations restrained to reflect the two-fold symmetry of the groups. The anisotropic displacement parameters of oxygen atoms O3X, O4X, O3Y, O4Y, O3Z and O4Z have been restrained to have isotropic behavior (ISOR).

The chemical identities of bridging ligands F, G and H could not be determined. It is likely that they are a disordered mixture of decomposition products of dimethylformamide and 1,4-dioxane, and all have been modeled as a full-occupancy oxygen atom bound to a full-occupancy carbon atom in turn bound to three half-occupancy carbon atoms. The oxygen atoms have been modeled anisotropically while all the carbon atoms have been modeled isotropically. The thermal displacement parameters of the half-occupied carbon atoms have been fixed at values of 0.075. The assumption of these species being a neutral species bridging via an oxygen atom is supported by a crystal structure of an otherwise identical molecule in which these positions are occupied by dimethylformamide ligands. The scattering contributions to these disordered fragments could not be removed by PLATON SQUEEZE as they are contiguous with the main residue. Further residual electron density peaks close to these ligands have not been modeled.

To give a charge-balanced structure required that 7 of the 11 oxygen atoms in the asymmetric unit be hydroxide ligands with the remainder being oxo ligands. Observation of hydrogen atom peaks in the

electron density map combined with longer Cd-O bond lengths confirmed the identity of 4 oxygen atoms as hydroxide ligands (O22, O29, O30, and O31). The hydrogen atoms for these ligands were geometrically placed to make an equal angle with each O-Cd bond (AFIX 13) and refined using a riding model. The location of the remaining three hydroxide groups could not be determined and were not included in the model but were included in the unit cell contents.

The contents of the large internal cavity of the molecule were disordered and could not be modeled. Consideration of the output of PLATON SQUEEZE (see below) indicated an electron count of 317 in a void of volume 880 A^3. These data are consistent with the cavity being occupied by 8 dimethylformamide molecules. Some large residual electron density peaks remain in the void even after refinement of the structure against the solvent free diffraction data generated by PLATON SQUEEZE.

PLATON SQUEEZE has been applied to the data to remove the scattering contribution from several disordered solvent moieties and produce a set of solvent-free diffraction intensities for the final cycles of refinement. A total of 8303 electrons were removed from the P1 cell, equating to around 26 dimethylformamide molecules per asymmetric unit which have been included in the unit cell contents.

Complex 2

Rigid bond and similarity restraints (DELU, SIMU) have been applied to the anisotropic displacement parameters of all the atoms in the structure. Geometric similarity restraints (SAME) have been applied to the three dimethylformamide molecules, which have each been restrained to lie in a plane (FLAT).

Water molecule O2W/O2W' was found to be disordered over two positions each of which were refined to have a half-occupancy. The separations between Cd1 and the two molecules were restrained to be approximately equal (SADI). The hydrogen atoms of the three water molecules in the structure could not be observed in the electron density map and so were not included in the refinement. Dimethylformamide molecule A is substitutionally disordered with water molecule O1W and orientationally disor-

dered with itself over a special position. The occupancies of the pair of molecules were refined and found to be approximately half for the water molecules and a quarter for each orientation of the dimethylformamide molecule. These values were subsequently fixed as such. The atoms of the dimethylformamide molecule could only be refined isotropically. The ADP of C4A was unexpectedly high compared to its neighbours and so was fixed to a comparable value of 0.15. The separations between Cd1 and the two coordinated oxygen atoms were restrained to be similar (SADI). Dimethyformamide molecule B is substitutionally disordered with water molecule O3W, and the occupancies of each molecules were refined and found to be approximately a half before being fixed as such. The separations between Cd2 and the two co-ordinated oxygen atoms were restrained to be equal (SADI). Oxygen atom O3W was refined isotropically. PLATON SQUEEZE has been applied to the data to remove the scattering contribution from several disordered solvent moieties and produce a set of solvent-free diffraction intensities for the final cycles of refinement. A total of 697 electrons was removed from the P1 cell, equating to around two dimethylformamide molecules per asymmetric unit which have been included in the unit cell contents.

Complex 3

All non-metal atoms in the structure have been refined with isotropic displacement parameters owing to a lack of high angle data as a result of weak diffraction from a small crystal. The resulting structure determination is of sufficient quality to confirm the identity of the components and the topology of the network formed.

Complex 4

The hydrogen atoms of dimethylamine ligand Y and dimethylammonium molecule Z were located in the electron difference map before being placed geometrically and refined using a riding model. The

structure was found to be racemically twinned with the major twin fraction being refined to a value of 0.379(6). The largest residual electron density peak of 1.91 e A^{-3} lies 0.91 A from Cd1 and is not indicative of an unmodeled chemical entity.

Atom	Obs	Obs-Avg	Assign	Atom	Obs	Obs-Avg	Assign
O23 -				O31 -			
Cd3	2.225	-0.030		Cd15	2.217	-0.038	
Cd2	2.231	-0.025		Cd14	2.279	0.024	
Cd17	2.239	-0.017		Cd20	2.387	0.132	
Avg	**2.232**	**-0.024**	**?**	**Avg**	**2.295**	**0.039**	**OH**
O24 -				O32 -			
Cd5	2.187	-0.069		Cd16	2.228	-0.027	
Cd4	2.203	-0.053		Cd15	2.233	-0.023	
Cd22	2.235	-0.021		Cd8	2.253	-0.003	
Avg	**2.208**	**-0.047**	**O**	**Avg**	**2.238**	**-0.018**	**?**
O25 -				O33 -			
Cd6	2.228	-0.028		Cd17	2.195	-0.060	
Cd5	2.284	0.028		Cd18	2.203	-0.052	
Cd22	2.405	0.150		Cd19	2.216	-0.039	
Avg	**2.305**	**0.050**	**OH**	**Avg**	**2.205**	**-0.051**	**O**
O26 -				O34 -			
Cd7	2.225	-0.030		Cd11	2.222	-0.034	
Cd6	2.231	-0.025		Cd18	2.295	0.040	
Cd4	2.239	-0.016		Cd21	2.374	0.119	
Avg	**2.232**	**-0.024**	**?**	**Avg**	**2.297**	**0.042**	**OH**
O27 -				O35 -			
Cd8	2.196	-0.060		Cd16	2.311	0.055	
Cd9	2.211	-0.044		Cd7	2.335	0.080	
Cd20	2.239	-0.017		Cd3	2.339	0.083	
Avg	**2.215**	**-0.040**	**O**	**Avg**	**2.328**	**0.073**	**OH**
O28 -				O36 -			
Cd2	2.229	-0.027		Cd12	2.325	0.069	
Cd9	2.268	0.013		Cd12	2.325	0.069	
Cd19	2.359	0.103		Cd12	2.325	0.069	
Avg	**2.285**	**0.030**	**OH**	**Avg**	**2.325**	**0.069**	**OH**
O29 -				O37 -			
Cd12	2.215	-0.041		Cd19	2.224	-0.032	
Cd11	2.230	-0.026		Cd21	2.239	-0.017	
Cd13	2.258	0.003		Cd20	2.243	-0.012	
Avg	**2.234**	**-0.021**	**?**	**Avg**	**2.235**	**-0.020**	**?**
O30 -				O38 -			
Cd13	2.177	-0.078		Cd22	2.243	-0.013	
Cd14	2.194	-0.062		Cd22	2.243	-0.013	
Cd21	2.250	-0.006		Cd22	2.243	-0.013	
Avg	**2.207**	**-0.049**	**O**	**Avg**	**2.243**	**-0.013**	**?**

Table S1. Observed bond lengths and deviations from average (2.255 Å) Cd-OH/O bond lengths in the crystal structure of **1**. The average values for each oxygen atom is given after its three individual values along with an assignment of either HO^- or O^{2-} , or in some instances the assignment remains ambiguous. Negative values are shown in red.

Atom	Obs	Obs-Avg	Assign	Atom	Obs	Obs-Avg	Assign
O21 -				O27 -			
Cd17	2.253	-0.001		Cd5	2.210	-0.044	
Cd16	2.253	-0.000		Cd11	2.220	-0.034	
Cd18	2.270	0.017		Cd17	2.236	-0.018	
Avg	**2.259**	**0.005**	**?**	**Avg**	**2.222**	**-0.032**	**O**
O22 -				O28 -			
Cd14	2.301	0.047		Cd13	2.193	-0.061	
Cd12	2.309	0.055		Cd7	2.230	-0.024	
Cd10	2.311	0.057		Cd18	2.243	-0.011	
Avg	**2.307**	**0.053**	**OH**	**Avg**	**2.222**	**-0.032**	**O**
O23 -				O29 -			
Cd4	2.228	-0.026		Cd4	2.202	-0.052	
Cd10	2.253	-0.001		Cd5	2.279	0.025	
Cd15	2.266	0.013		Cd16	2.344	0.091	
Avg	**2.249**	**-0.005**	**?**	**Avg**	**2.275**	**0.021**	**OH**
O24 -				O30 -			
Cd6	2.234	-0.020		Cd6	2.209	-0.045	
Cd11	2.257	0.004		Cd7	2.268	0.014	
Cd12	2.262	0.009		Cd17	2.336	0.083	
Avg	**2.251**	**-0.003**	**?**	**Avg**	**2.271**	**0.017**	**OH**
O25 -				O31 -			
Cd14	2.228	-0.025		Cd8	2.235	-0.019	
Cd8	2.245	-0.009		Cd9	2.271	0.018	
Cd13	2.247	-0.006		Cd18	2.317	0.063	
Avg	**2.240**	**-0.014**	**?**	**Avg**	**2.274**	**0.021**	**OH**
O26 -							
Cd9	2.216	-0.038					
Cd15	2.219	-0.035					
Cd16	2.243	-0.011					
Avg	**2.226**	**-0.028**	**O**				

Table S2. Observed bond lengths and deviations from average (2.254 Å) Cd-OH/O bond lengths in the crystal structure of **1a**. The average values for each oxygen atom is given after its three individual values along with an assignment of either HO^- or O^{2-}, or in some instances the assignment remains ambiguous. Negative values are shown in red.

Group	Type	Donor	Dist	Type	Donor	Dist	Type	Donor	Dist	Type	Donor	Dist
i		**Cd2**			**Cd6**			**Cd11**			**Cd15**	
	C	O78E	2.196	**N**	O4X	2.204	**C**	O58F	2.195	**H**	O31	2.217
	?	O23	2.225	**?**	O26	2.225	**H**	O34	2.222	**N**	O4Z	2.218
	H	O28	2.229	**C**	O58C	2.226	**?**	O29	2.230	**?**	O32	2.233
	N	O4W	2.233	**H**	O25	2.228	**N**	O4Y	2.255	**C**	O38D	2.252
	C	O38E	2.345	**C**	O78C	2.312	**C**	O78F	2.333	**C**	O58D	2.343
	C	O58E	2.355	**C**	O38C	2.334	**C**	O38F	2.375	**C**	O78D	2.349
ii		**Cd3**			**Cd7**			**Cd12**			**Cd16**	
	C	O79E	2.218	**?**	O26	2.231	**C**	O59F	2.207	**?**	O32	2.228
	?	O23	2.231	**C**	O59C	2.240	**?**	O29	2.215	**C**	O39D	2.240
	C	O58B	2.313	**C**	O38B	2.323	**C**	O38G	2.319	**H**	O35	2.311
	H	O35	2.339	**H**	O35	2.335	**H**	O36	2.325	**N**	O2Z	2.340
	N	O2W	2.346	**N**	O2X	2.340	**N**	O2Y	2.348	**C**	O78B	2.344
	C	O78B	2.405	**C**	O58B	2.387	**C**	O38G	2.419	**C**	O38B	2.387
iii		**Cd4**			**Cd8**			**Cd13**			**Cd17**	
	O	O24	2.203	**C**	O39B	2.186	**O**	O30	2.177	**C**	O79B	2.198
	C	O59B	2.225	**O**	O27	2.196	**C**	O39G	2.199	**O**	O33	2.203
	?	O26	2.239	**?**	O32	2.253	**?**	O29	2.258	**?**	O23	2.239
	N	O2W	2.304	**N**	O2X	2.313	**N**	O2Y	2.297	**N**	O2Z	2.309
	D	O1I	2.377	**D**	O1J	2.411	**D**	O1K	2.424	**D**	O1L	2.394
	C	O38C	2.506	**C**	O78D	2.525	**C**	O38F	2.484	**C**	O58E	2.456
iv		**Cd5**			**Cd9**			**Cd14**			**Cd18**	
	O	O24	2.187	**O**	O27	2.211	**O**	O30	2.194	**O**	O33	2.195
	C	O39H	2.201	**C**	O59A	2.219	**C**	O79A	2.199	**N**	O3Z	2.206
	N	O3W	2.211	**N**	O3X	2.225	**N**	O3Y	2.209	**C**	O39A	2.213
	H	O25	2.284	**H**	O28	2.268	**H**	O31	2.279	**H**	O34	2.295
	C	O78C	2.430	**C**	O38E	2.392	**C**	O58D	2.384	**C**	O78F	2.374
	D	O1I	2.631	**D**	O1J	2.612	**D**	O1K	2.585	**D**	O1L	2.595
v		**Cd19**			**Cd20**			**Cd21**			**Cd22**	
	O	O33	2.216	**C**	O79D	2.238	**?**	O37	2.239	**C**	O39C	2.233
	?	O37	2.224	**O**	O27	2.239	**C**	O39F	2.242	**O**	O24	2.235
	C	O59E	2.238	**?**	O37	2.243	**O**	O30	2.250	**?**	O38	2.243
	C	O58A	2.344	**C**	O78A	2.335	**C**	O38A	2.318	**C**	O38H	2.345
	H	O28	2.359	**H**	O31	2.387	**H**	O34	2.374	**H**	O25	2.405
	C	O38A	2.436	**C**	O58A	2.440	**C**	O78A	2.462	**C**	O38H	2.452
vi		**Cd1**			**Cd10**							
	C	O39E	2.224	**C**	O79F	2.238						
	C	O79C	2.258	**C**	O59D	2.250						
	N	O3W	2.308	**N**	O3Y	2.309						
	N	O4X	2.319	**N**	O3Z	2.316						
	N	O4W	2.332	**N**	O4Z	2.326						
	N	O3X	2.339	**N**	O4Y	2.334						

Table S3. Observed Cd-O bond lengths in the crystal structure of **1**. The 22 crystallographically unique Cd(II) centers are grouped (horizontally) into six groups (i-vi) with identical idealised symmetry. Distances (Å) are preceded by donor name and donor type (types: C carboxylate; N nitrate; D DMF; O oxo; H hydroxide; ? ambiguous HO^-/O^{2-}). Donors are listed in order of increasing bond length.

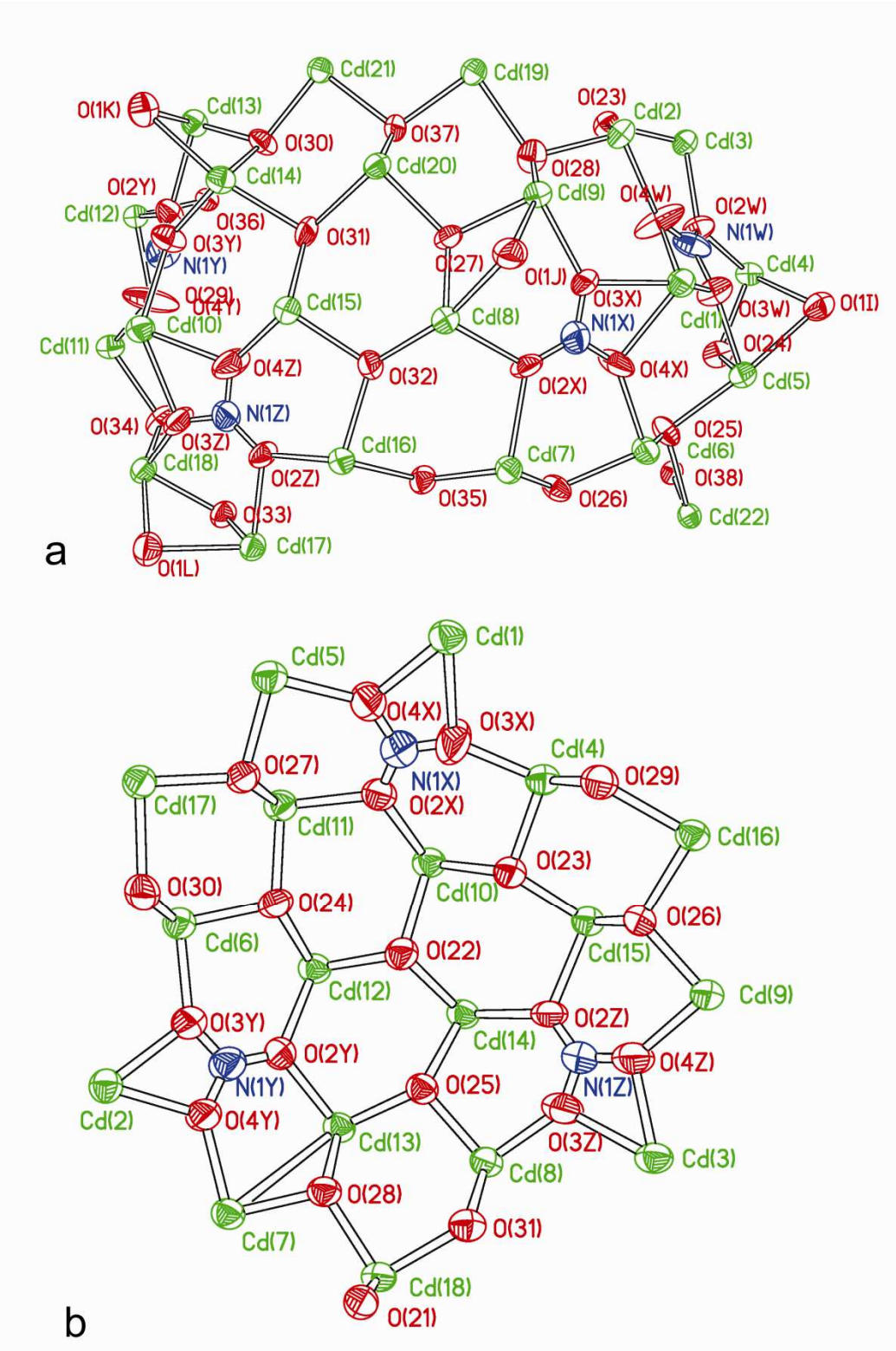

Fig. S5 Thermal ellipsoid plots (50% probability) of the asymmetric units of a) **1** and b) **1a** with hydrogen atoms, carboxylate ligands and DMF ligands omitted for clarity.

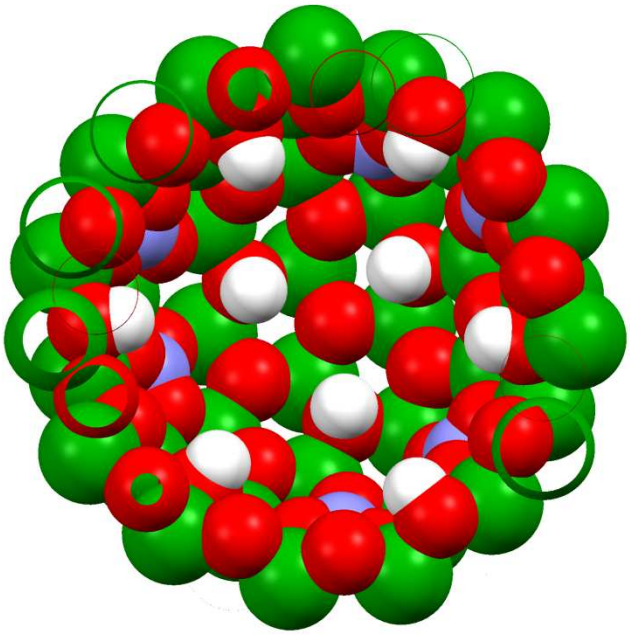

Fig. S6 Cutaway space-filling view of the interior of the metallo-core of **1** showing the HO^- hydrogen atoms (white) pointing into the center of the cavity. Hydrogen white; Nitrogen blue; Oxygen red; Cadmium green.

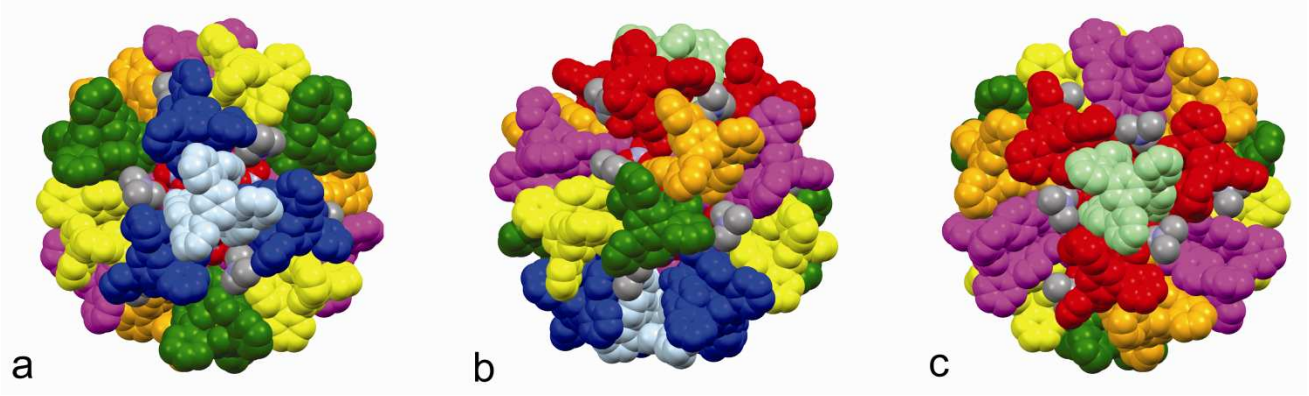

Fig. S7 Alternative space filling views of **1** a) up, b) perpendicular to and c) down the three fold axis with ligands colored to indicate their crystallographic symmetry (colors: A yellow; B orange; C red; D green; E purple; F blue; G pale blue; H pale green; DMF grey).

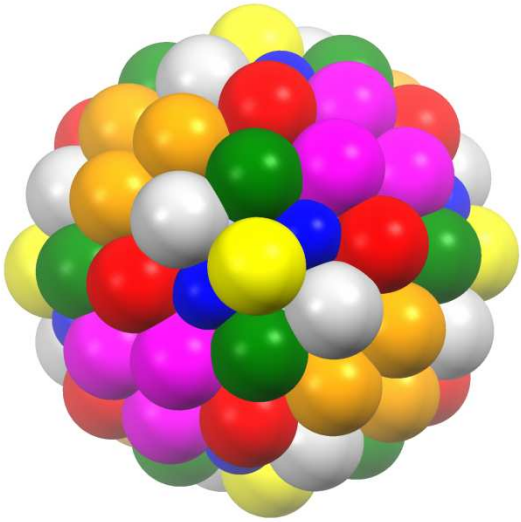

Fig. S8 Space filling view of **1** showing only Cd(II) cations and nitrate nitrogen atoms colored to denote idealized symmetry groups (see Table S3). Colors: i green; ii pink; iii red; iv grey; v orange; vi yellow.

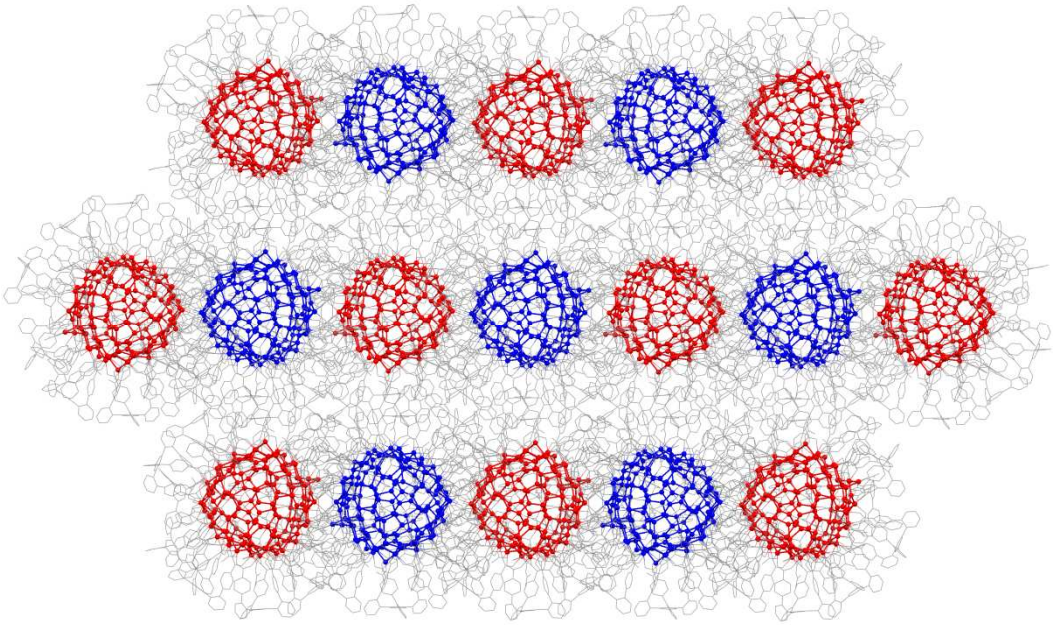

Fig. S9 Packing of **1** viewed perpendicular to the (110) plane with metallo-cores colored red or blue, all other atoms are grey and hydrogen atoms omitted. The like colored molecules are co-planar with the plane of blue molecules lying above the red ones.

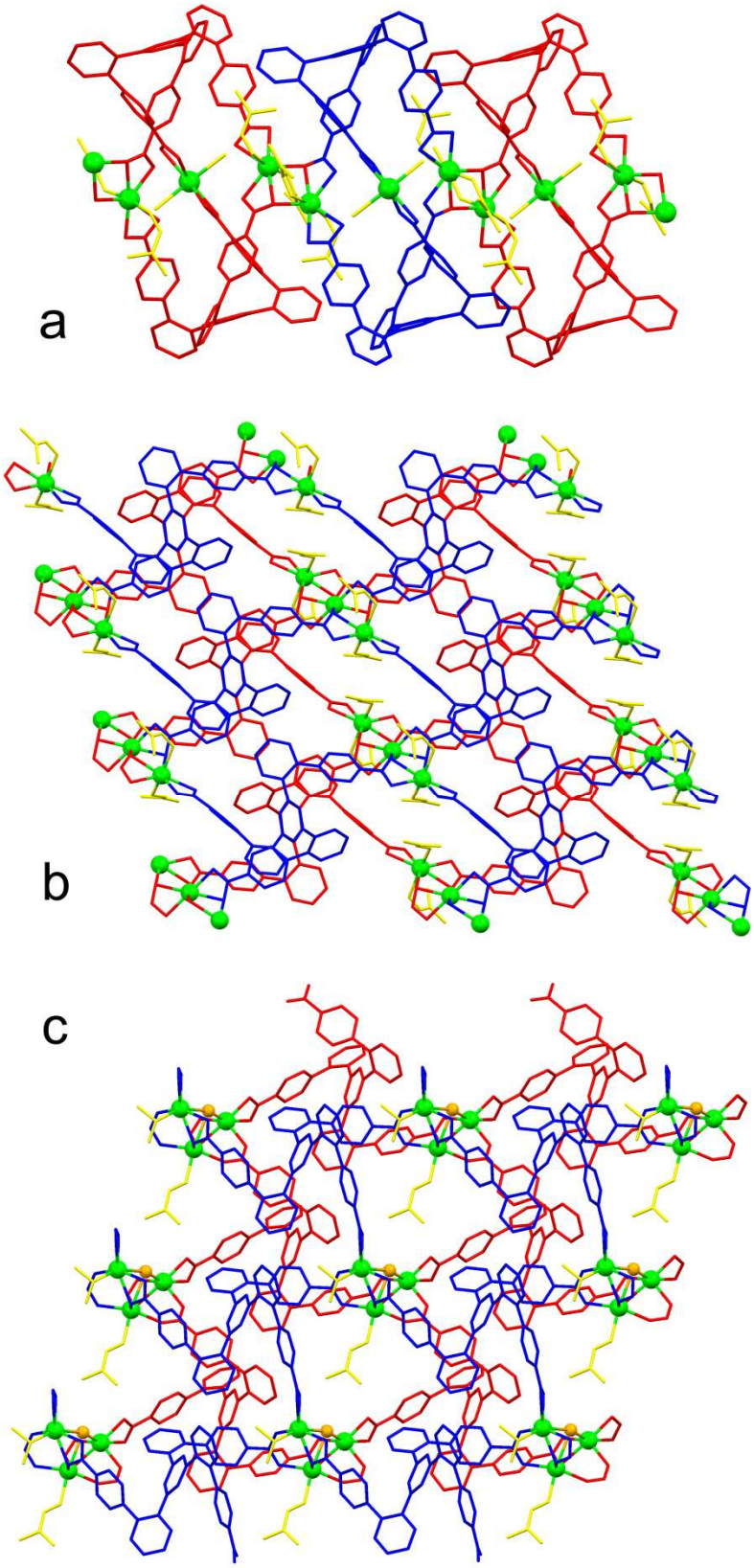

Fig. S10 View of the extended one dimensional networks of a) **2,** b) **3** and c) **4**. Colors: ligand red or blue; cadmium atoms green; dimethylformamide, dimethylamine and water molecules yellow.

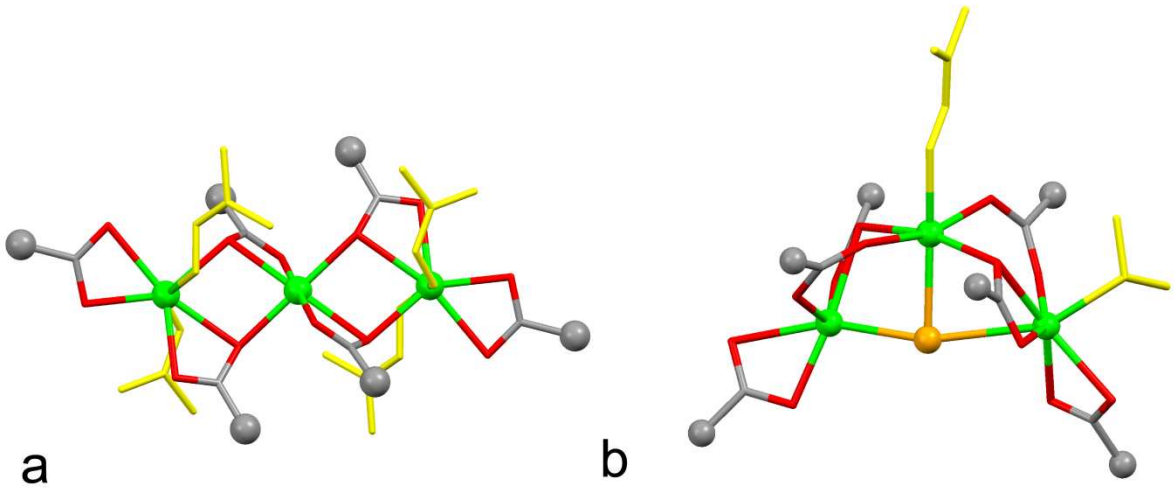

Fig. S11 View of the cluster building-blocks observed a) $[Cd_3(RCO_2)_6(DMF)_4]$ in **3** and b) $[Cd_3Cl(RCO_2)_6(DMF)(DMA)]$ in **4**. Colors: carbon atoms grey; oxygen atoms red; cadmium atoms green; chlorine atoms orange; dimethylformamide and dimethylamine molecules yellow.

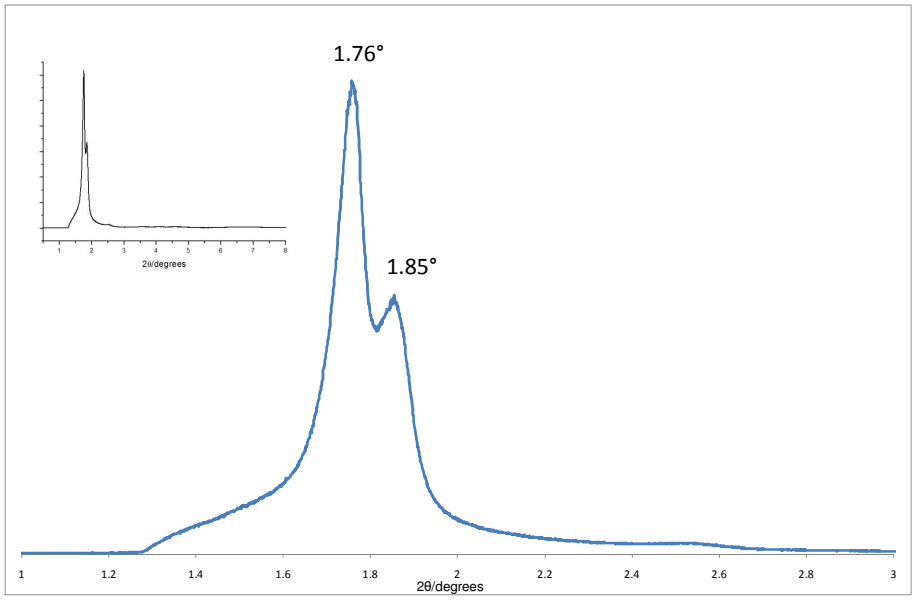

Fig. S12 PXRD pattern of a dried and ground sample of **1** (λ = 0.82613 Å).

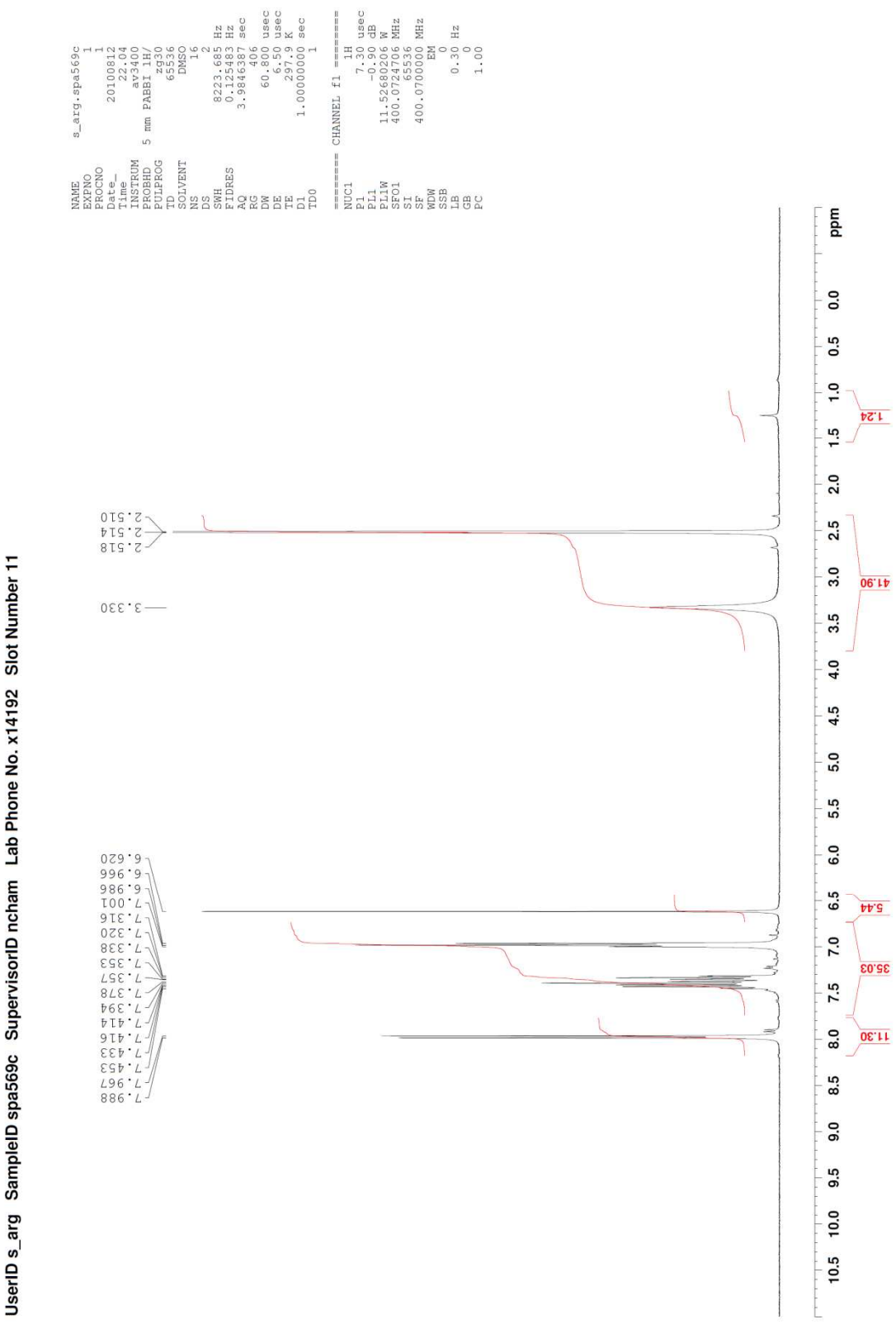

Fig. S13 ^{1}H-NMR spectrum (DMSO-d_6, 400 MHz) of **7**

Fig. S14 ^{1}H-NMR spectrum (CD_2Cl_2, 500 MHz) of **1** with single solvent pre-saturation at 5.36 ppm.

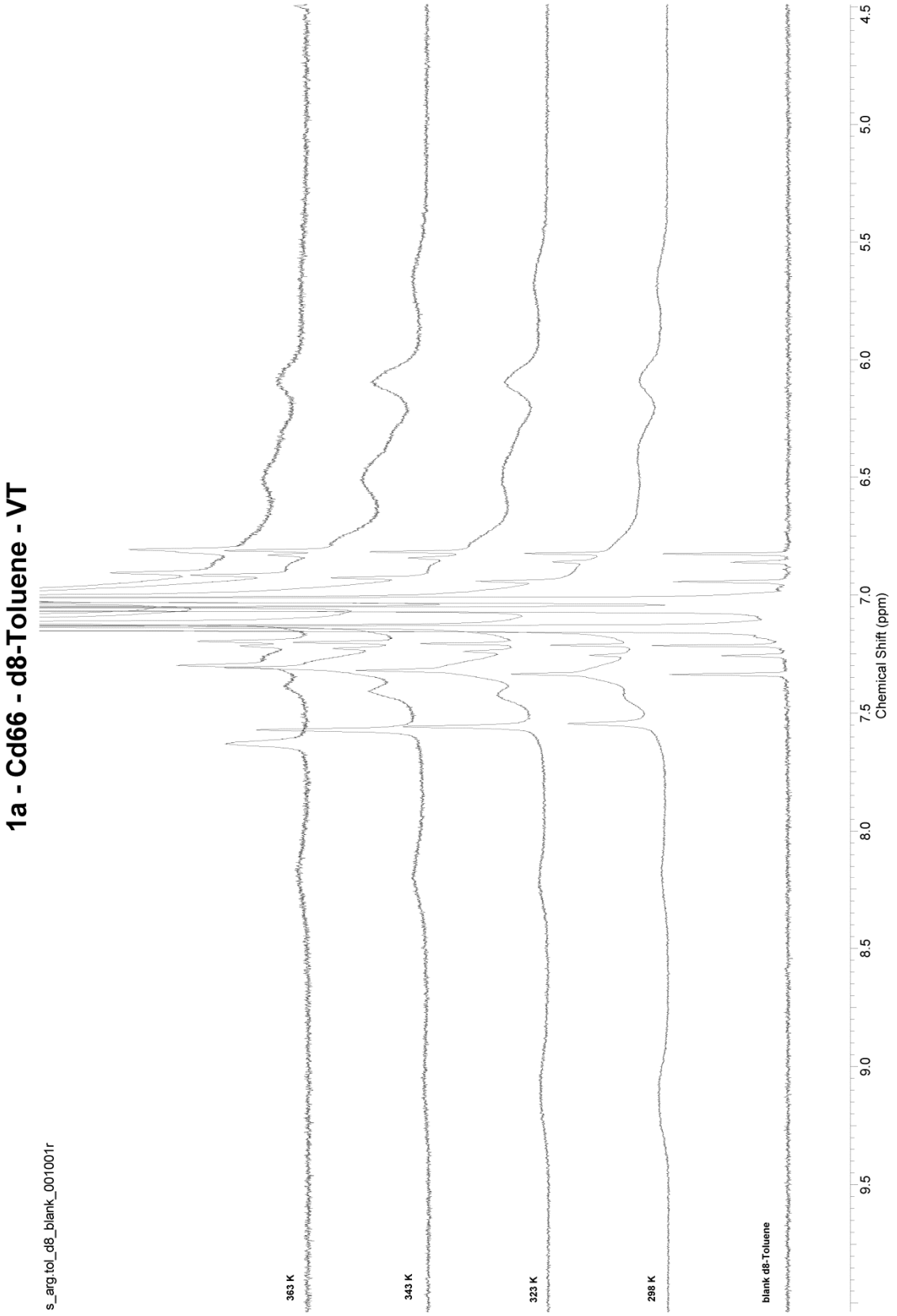

Fig. S15 Variable Temperature ^{1}H-NMR spectrum (d8-Toluene, 400 MHz) of **1**.

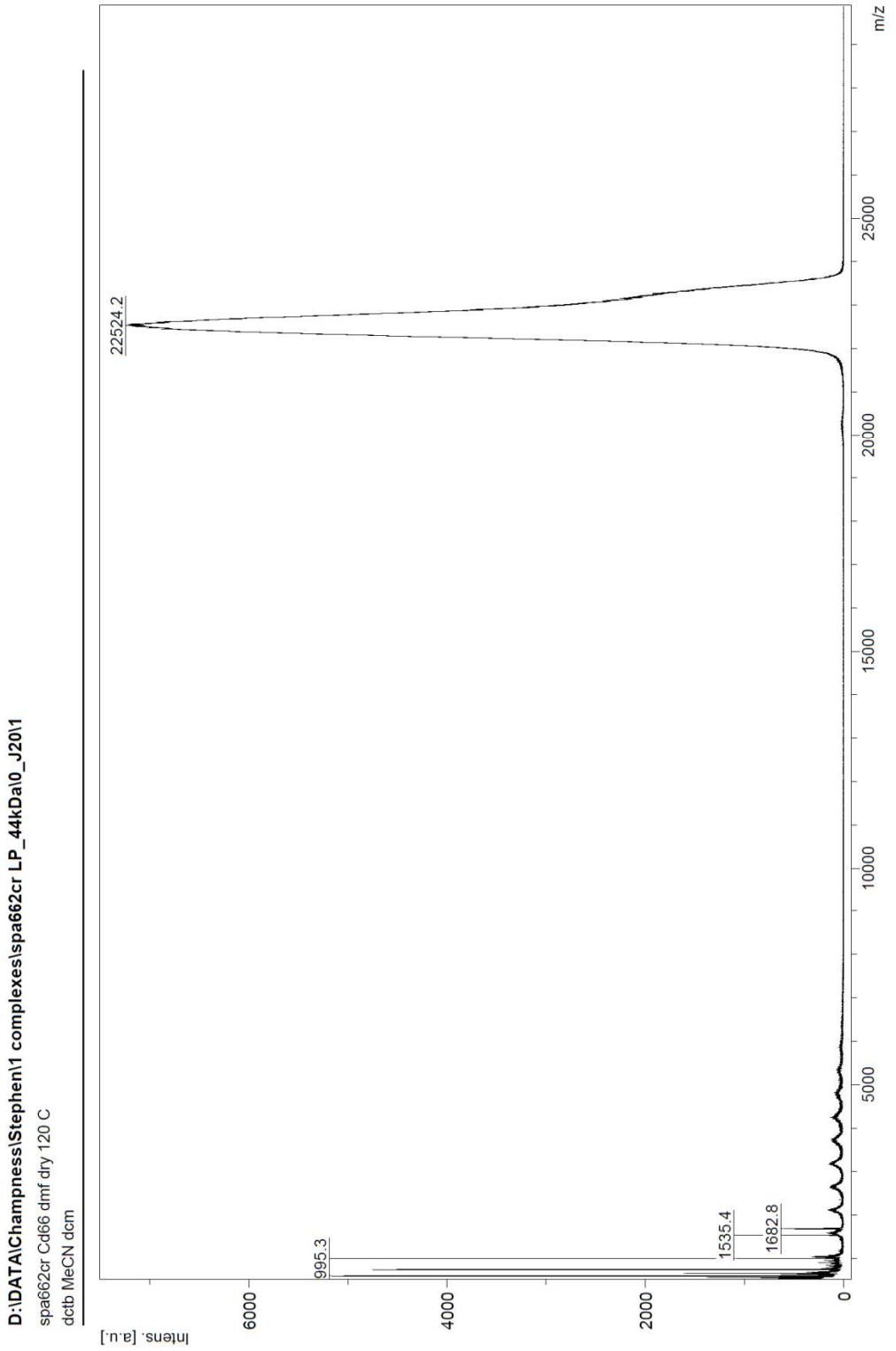

Fig. S16 MALDI-MS of **1** at full range.

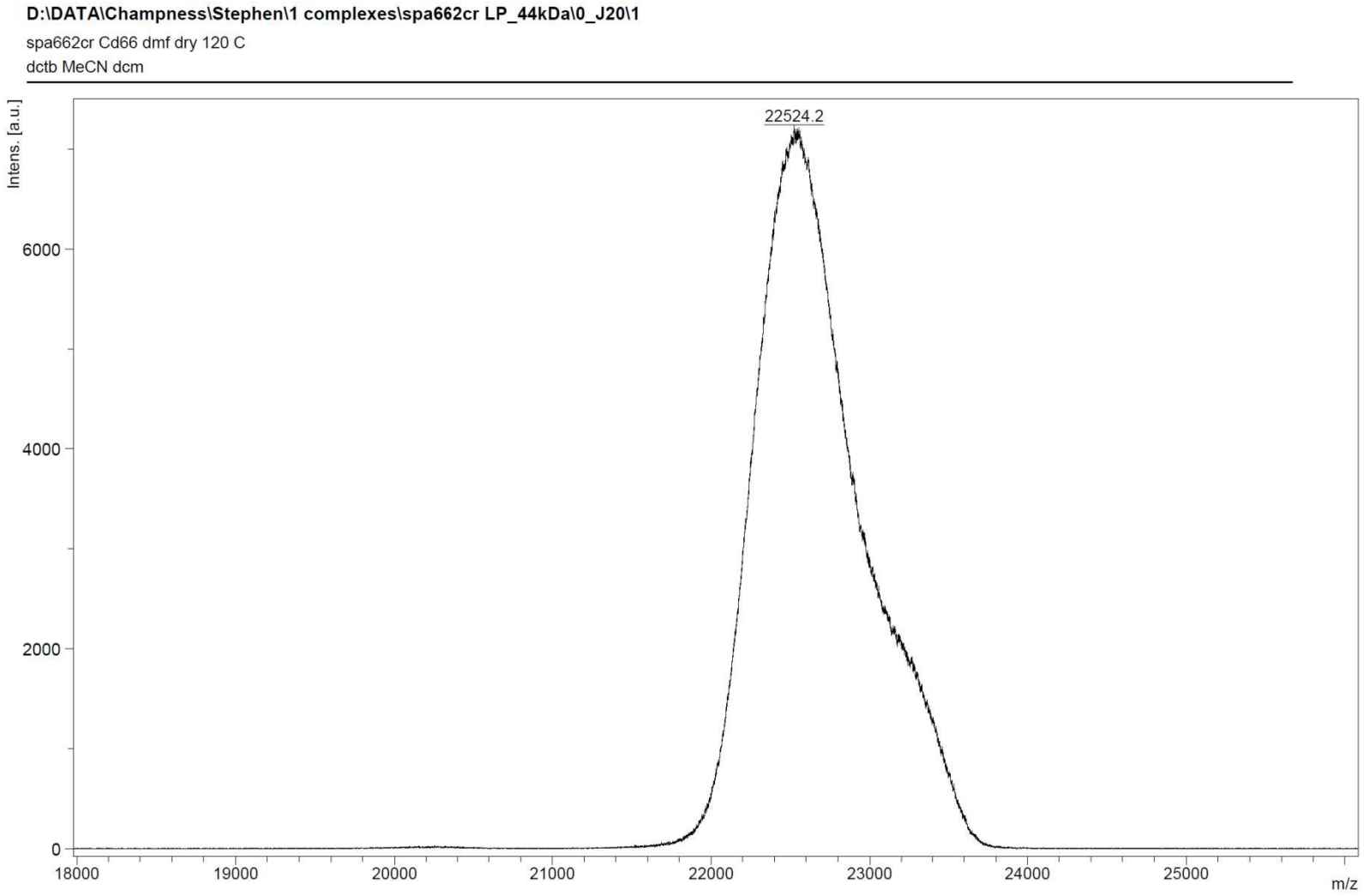
D:\DATA\Champness\Stephen\1 complexes\spa662cr LP_44kDa\0_J20\1
spa662cr Cd66 dmf dry 120 C
dctb MeCN dcm
22524.2
Intens. [a.u.]
6000
4000
2000
0
18000
19000
20000
21000
22000
23000
24000
25000
m/z

Fig. S17 MALDI-MS of **1** at high *m/z* range.

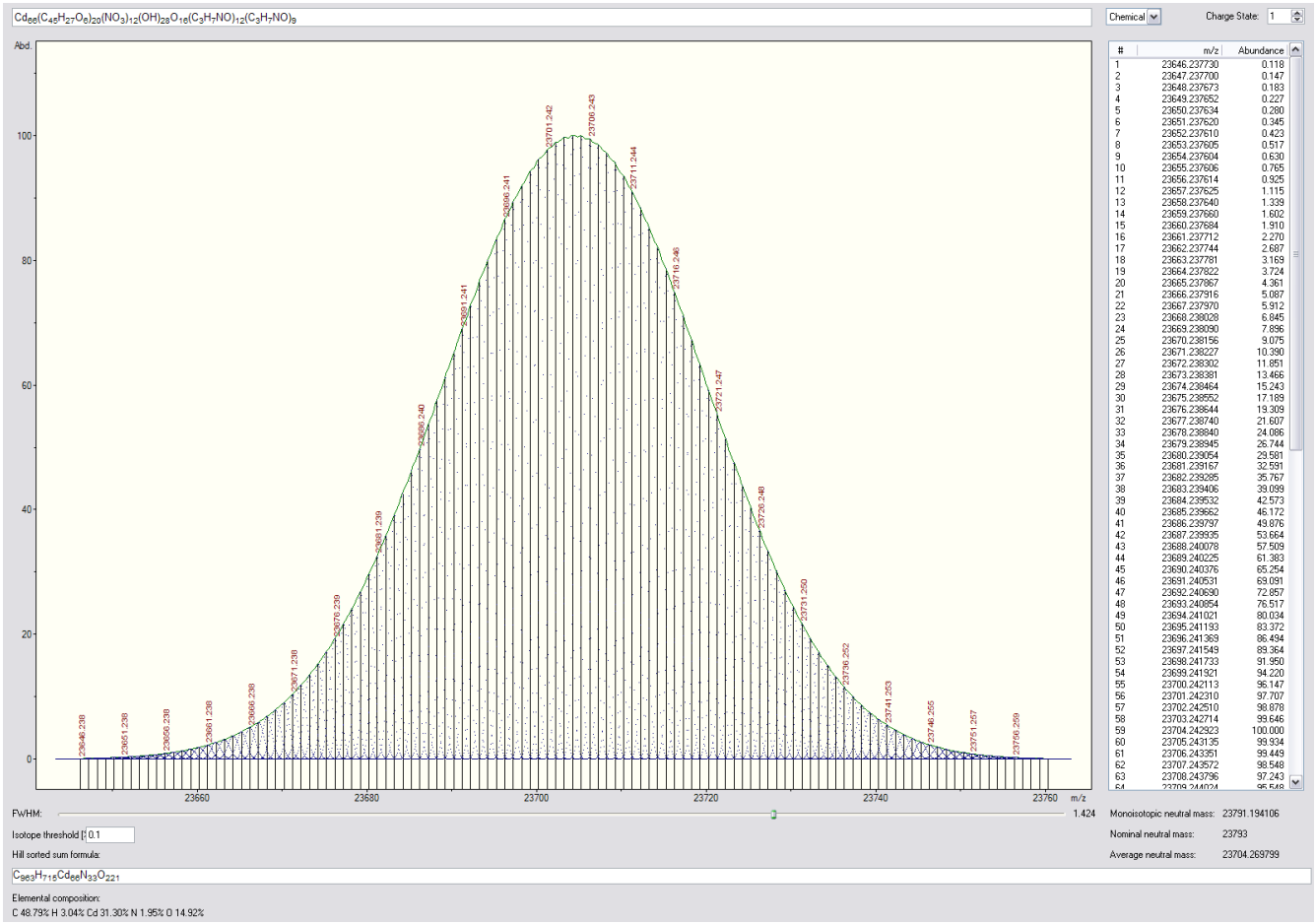

Fig. S18 Isotopic distribution pattern simulation for **1**.